Central Schemes: a Powerful Black-Box-Solver for Nonlinear Hyperbolic PDEs

Alexander Kurganov

Southern University of Science and Technology, China

and Tulane University, USA

www.math.tulane.edu/∼kurganov

Supported by NSF and NSFC

joint work with

Chi-Tien Lin, Providence University, Taiwan

Sebastian Noelle, University of Technology at Aachen, Germany

Guergana Petrova, Texas A&M University, USA

Martina Prugger, University of Innsbruck, Austria

Eitan Tadmor, University of Maryland, USA

Tong Wu, Tulane University, USA

Southern University of Science and Technology

Shenzhen (Special Economic Zone)

Population: 20,000 (1980), 15,000,000 (2018)

GDP per capita: Shenzhen 27,000$; China 16,000$
Nanshan District 50,000$ (higher than in Germany, Canada, Japan)

SUSTech is the first "Western" major research university in China founded in 2011

Department of Mathematics was founded in 2015

`http://math.sustc.edu.cn/?lang=en`

Size: 25 faculty (2018), 45-50 (within 3-5 years)

Many tenure/tenure-track, long and short term visiting, post-doc and PhD positions are available

Finite-Volume Methods

1-D System: $\boldsymbol{q}_t + \boldsymbol{f}(\boldsymbol{q})_x = 0$

Integrate it over the space-time control volumes $[a, b] \times [t^n, t^{n+1}]$ to obtain the integral form:

$$\int_a^b \boldsymbol{q}(x, t^{n+1})\, dx = \int_a^b \boldsymbol{q}(x, t^n)\, dx - \int_{t^n}^{t^{n+1}} \Big[\boldsymbol{f}(\boldsymbol{q}(b,t)) - \boldsymbol{f}(\boldsymbol{q}(a,t))\Big] dt$$

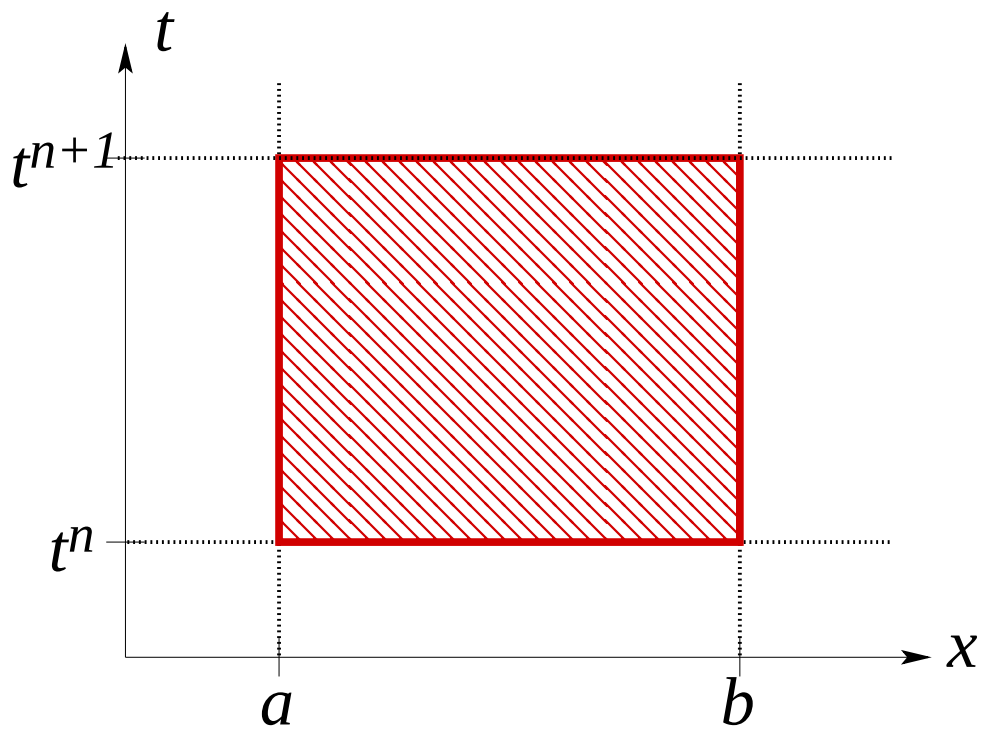

$\bar{\boldsymbol{q}}_j^n \approx \dfrac{1}{\Delta x} \displaystyle\int_{C_j} \boldsymbol{q}(x, t^n)\, dx$: cell averages over $C_j := (x_{j-\frac{1}{2}}, x_{j+\frac{1}{2}})$

This solution is approximated by a piecewise linear (conservative, second-order accurate, non-oscillatory) reconstruction:

$\tilde{\boldsymbol{q}}^n(x) = \bar{\boldsymbol{q}}_j^n + (\boldsymbol{q}_x)_j^n (x - x_j)$ for $x \in C_j$

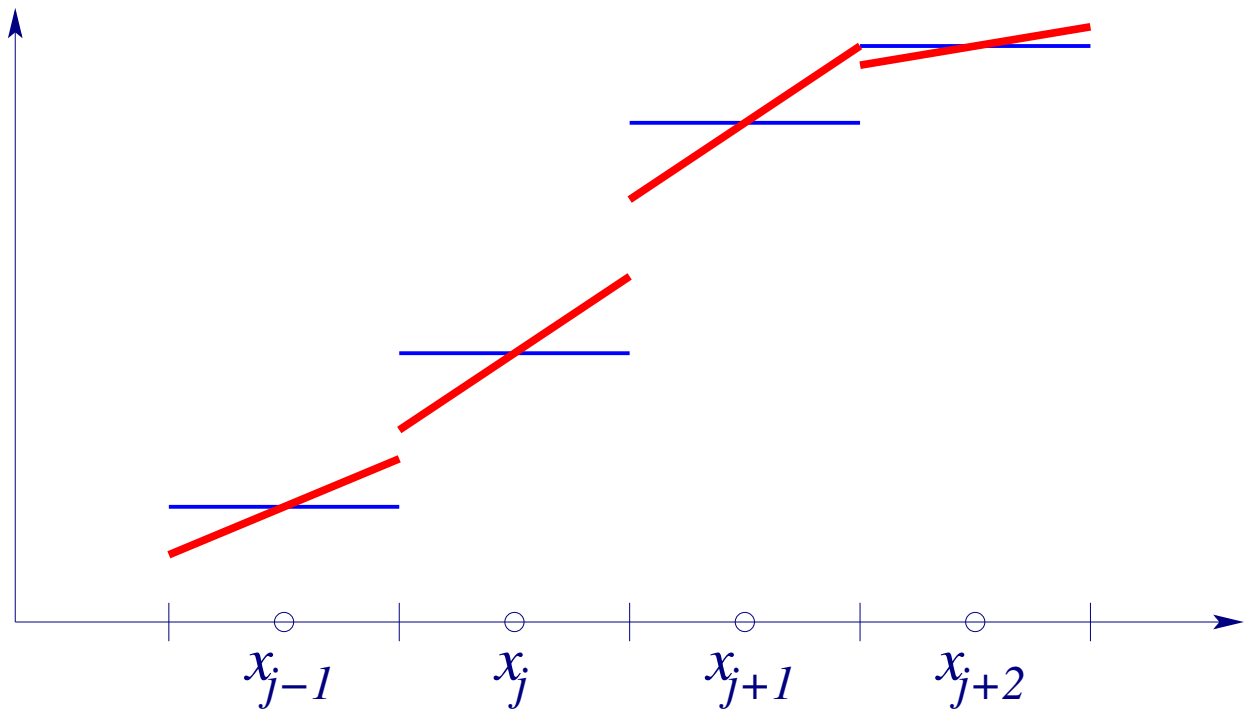

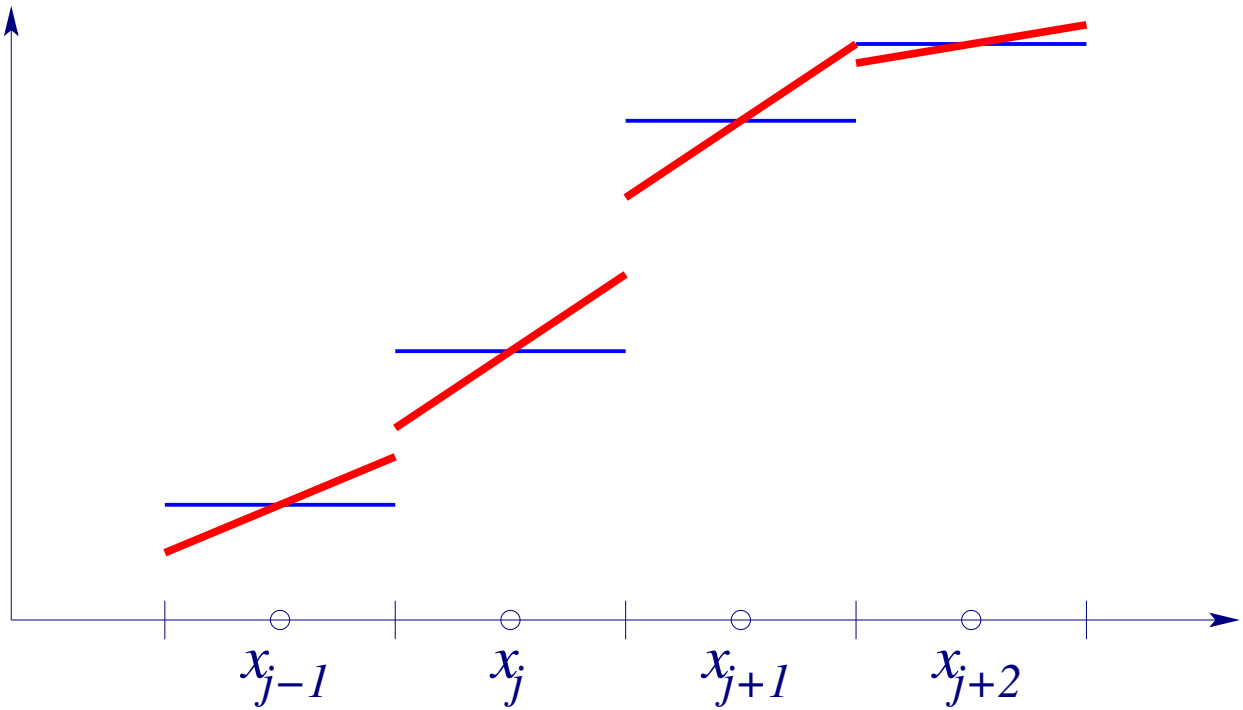

For example,

$$\boxed{(\boldsymbol{q}_x)_j^n = \text{minmod}\left(\theta\,\frac{\bar{\boldsymbol{q}}_j^n - \bar{\boldsymbol{q}}_{j-1}^n}{\Delta x},\ \frac{\bar{\boldsymbol{q}}_{j+1}^n - \bar{\boldsymbol{q}}_{j-1}^n}{2\Delta x},\ \theta\,\frac{\bar{\boldsymbol{q}}_{j+1}^n - \bar{\boldsymbol{q}}_j^n}{\Delta x}\right)} \quad \theta \in [1,2]$$

where the minmod function is defined as:

$$\boxed{\text{minmod}(z_1, z_2, \ldots) := \begin{cases} \min_j\{z_j\}, & \text{if} \quad z_j > 0 \quad \forall j \\ \max_j\{z_j\}, & \text{if} \quad z_j < 0 \quad \forall j \\ 0, & \text{otherwise} \end{cases}}$$

Godunov-type upwind schemes are designed by integrating

$$\boldsymbol{q}_t + \boldsymbol{f}(\boldsymbol{q})_x = \mathbf{0}$$

over the space-time control volumes $[x_{j-\frac{1}{2}}, x_{j+\frac{1}{2}}] \times [t^n, t^{n+1}]$

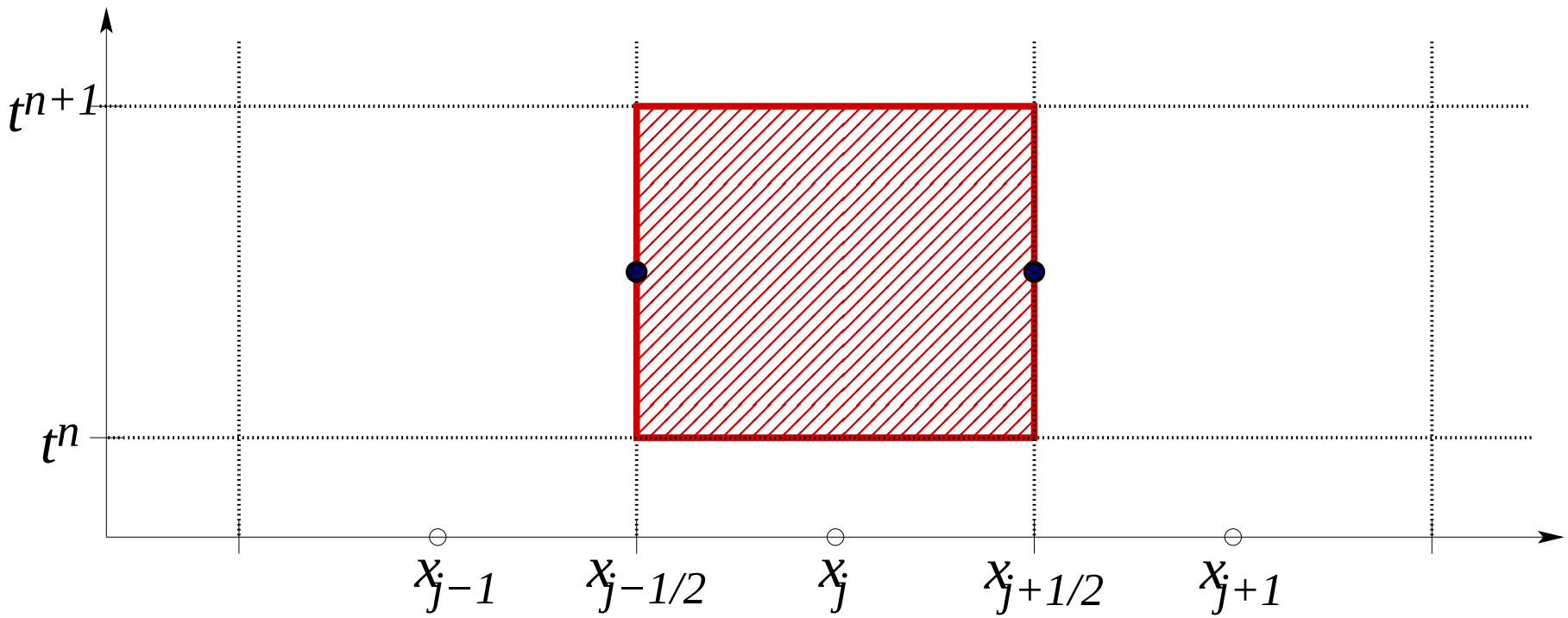

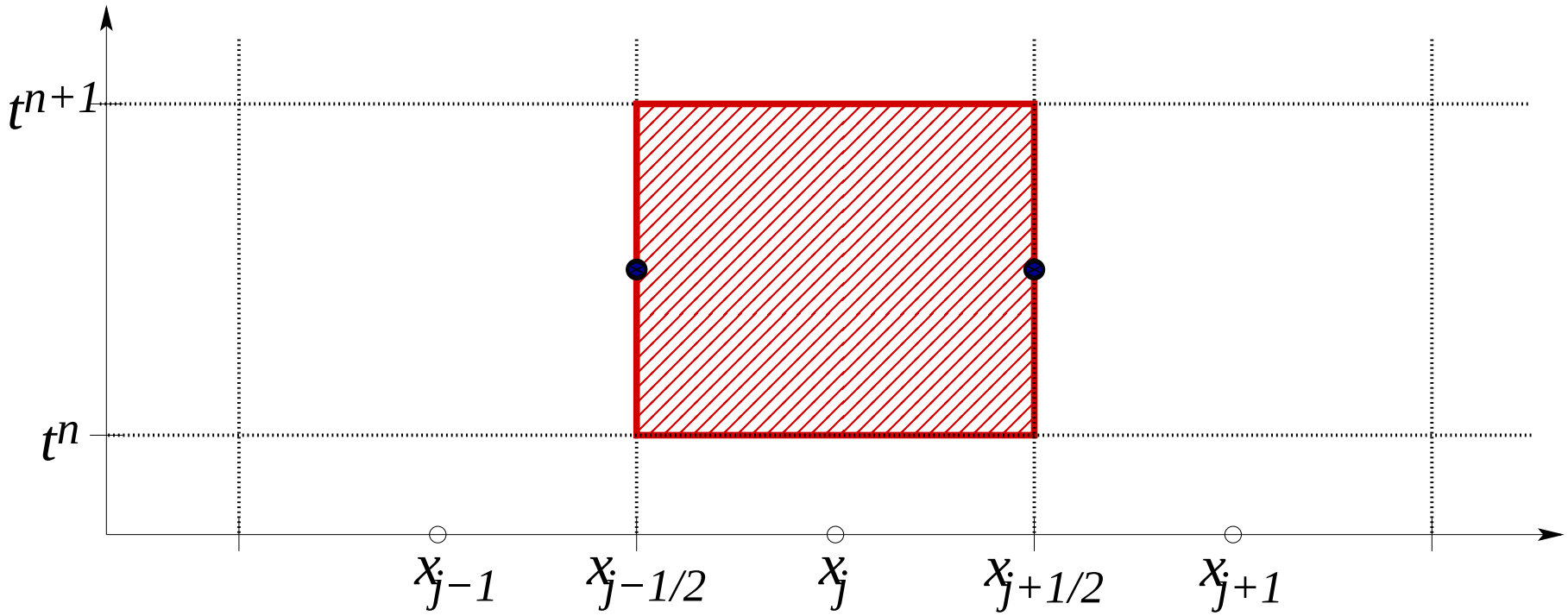

$$\bar{\boldsymbol{q}}_j^{n+1} = \bar{\boldsymbol{q}}_j^n - \frac{1}{\Delta x} \int_{t^n}^{t^{n+1}} \left[\boldsymbol{f}(\boldsymbol{q}(x_{j+\frac{1}{2}}, t)) - \boldsymbol{f}(\boldsymbol{q}(x_{j-\frac{1}{2}}, t)) \right] dt$$

In order to evaluate the flux integrals on the RHS, one has to (approximately) solve the generalized Riemann problem.

This may be hard or even impossible...

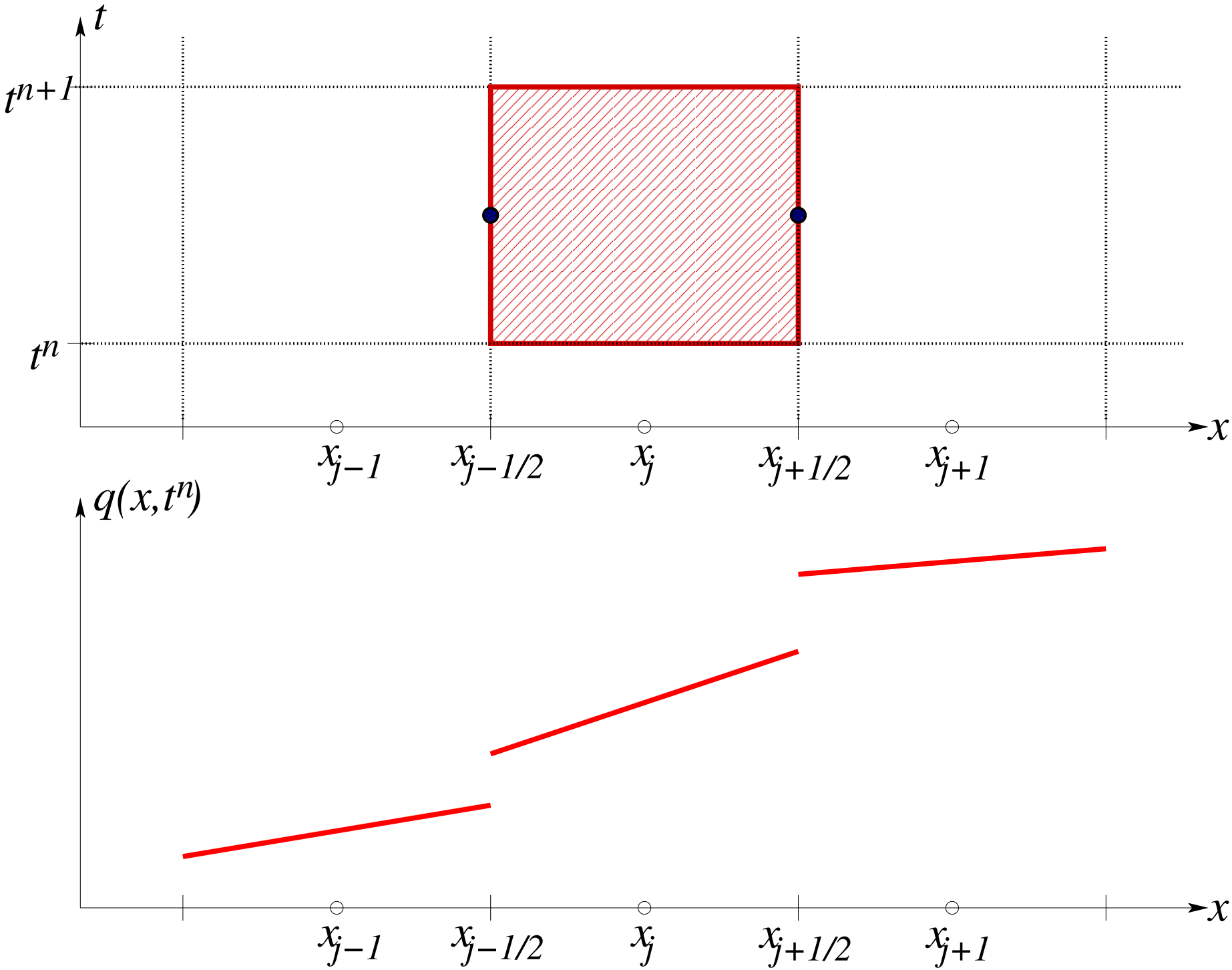
t
t^{n+1}
t^n
x
x_{j-1}
$x_{j-1/2}$
x_j
$x_{j+1/2}$
x_{j+1}
$q(x,t^n)$
x
x_{j-1}
$x_{j-1/2}$
x_j
$x_{j+1/2}$
x_{j+1}

Nessyahu-Tadmor Scheme

The Nessyahu-Tadmor [Nessyahu, Tadmor; 1990] scheme is a Godunov-type central scheme. It is designed by integrating

$$\boldsymbol{q}_t + \boldsymbol{f}(\boldsymbol{q})_x = \mathbf{0}$$

over the different set of staggered space-time control volumes $[x_j, x_{j+1}] \times [t^n, t^{n+1}]$ containing the Riemann fans

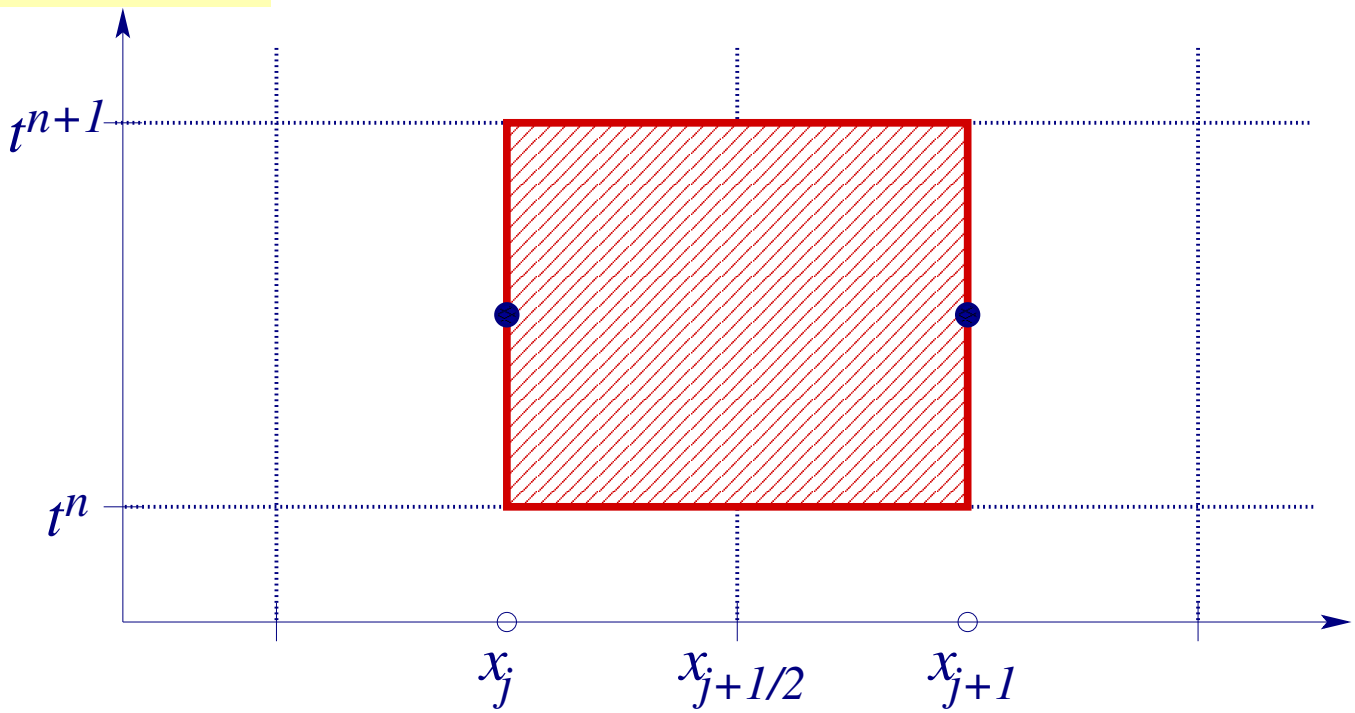

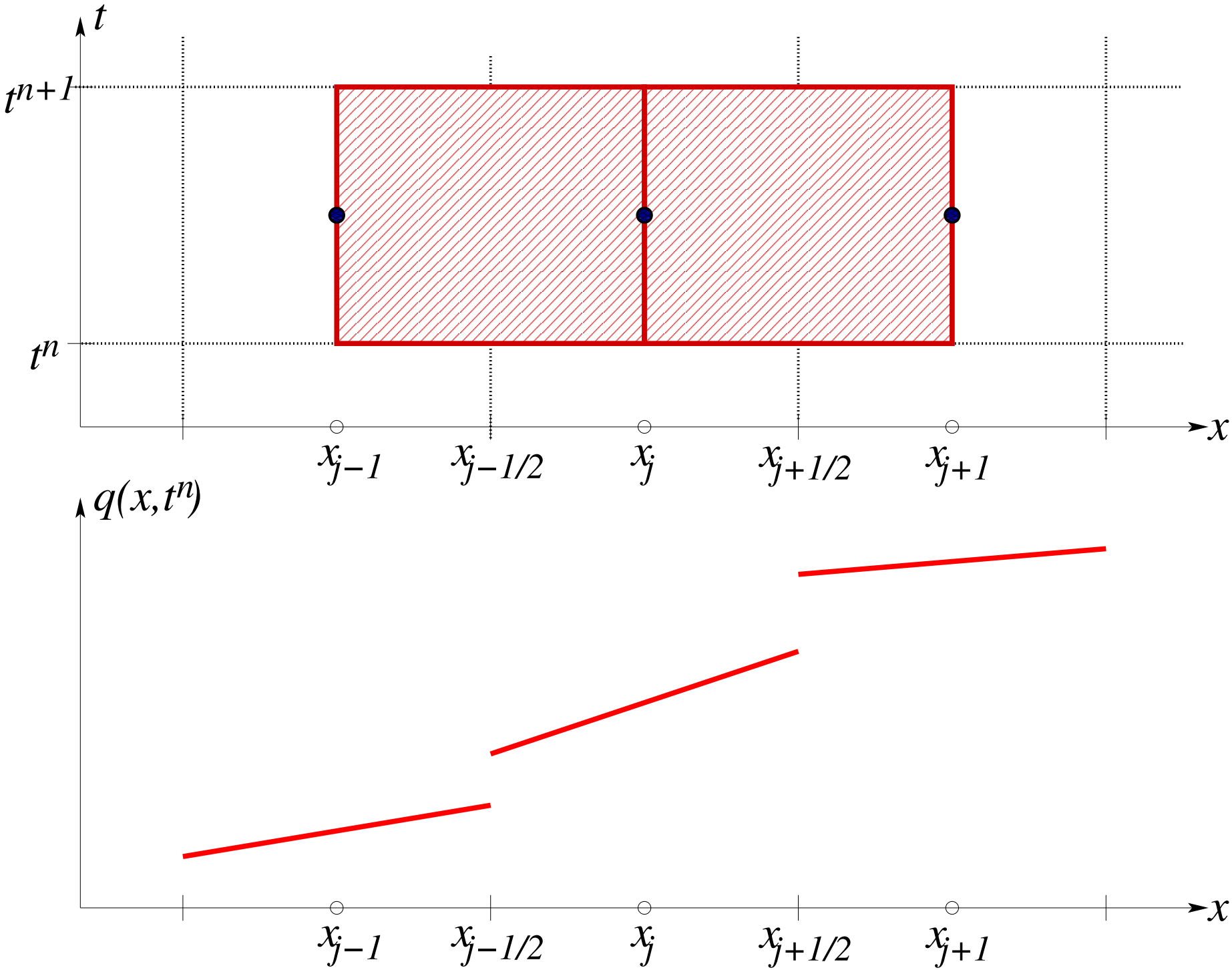
t
t^{n+1}
t^n
x
x_{j-1}
$x_{j-1/2}$
x_j
$x_{j+1/2}$
x_{j+1}
$q(x,t^n)$
x
x_{j-1}
$x_{j-1/2}$
x_j
$x_{j+1/2}$
x_{j+1}

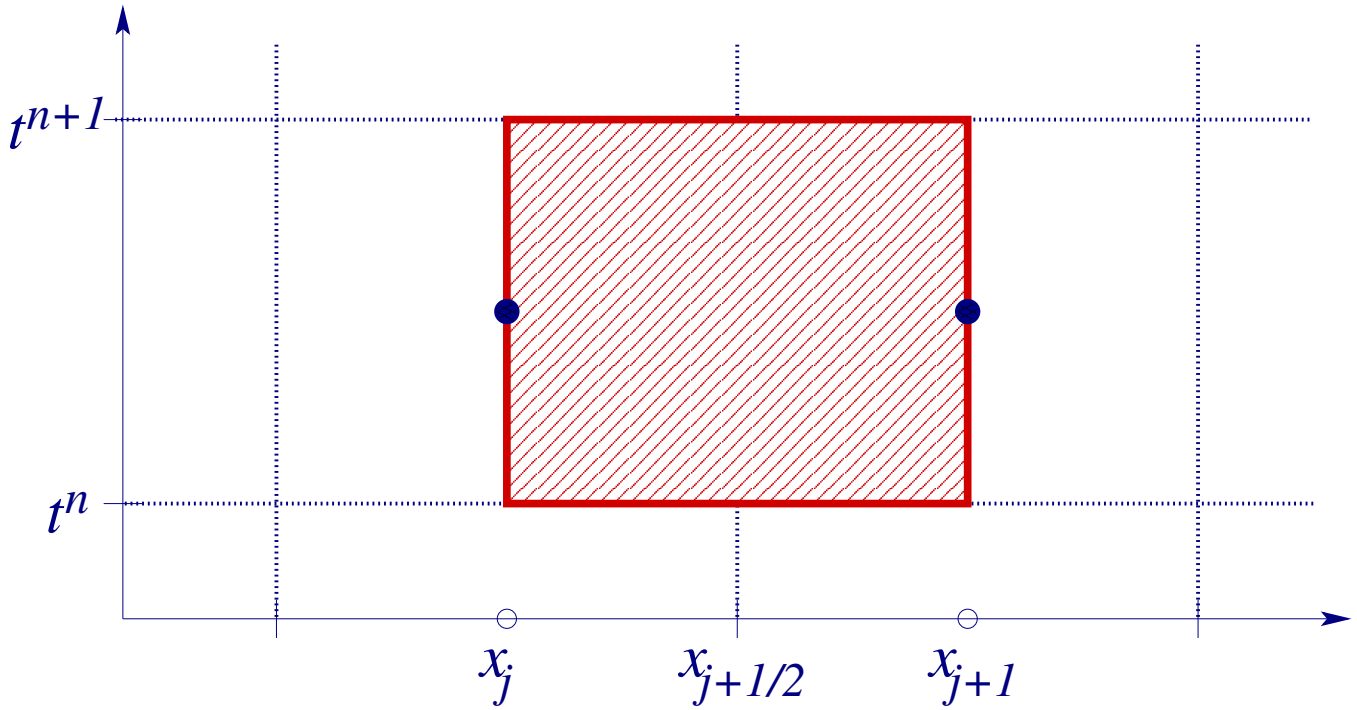

$$\bar{\boldsymbol{q}}_{j+\frac{1}{2}}^{n+1} = \frac{1}{\Delta x}\int_{x_j}^{x_{j+1}} \tilde{\boldsymbol{q}}^n(x)\,dx - \frac{1}{\Delta x}\int_{t^n}^{t^{n+1}} \Big[\boldsymbol{f}(\boldsymbol{q}(x_{j+1},t)) - \boldsymbol{f}(\boldsymbol{q}(x_j,t))\Big]dt$$

Due to the finite speed of propagation, this can be reduced to:

$$\bar{\boldsymbol{q}}_{j+\frac{1}{2}}^{n+1} = \frac{\bar{\boldsymbol{q}}_j^n + \bar{\boldsymbol{q}}_{j+1}^n}{2} + \frac{\Delta x}{8}\Big((\boldsymbol{q}_x)_j^n - (\boldsymbol{q}_x)_{j+1}^n\Big) - \frac{\Delta t}{\Delta x}\Big[\boldsymbol{f}(\boldsymbol{q}_{j+1}^{n+\frac{1}{2}}) - \boldsymbol{f}(\boldsymbol{q}_j^{n+\frac{1}{2}})\Big]$$

Values of $\boldsymbol{q}$ at $t = t^{n+\frac{1}{2}}$ are approximated using the Taylor expansion:

$$\boldsymbol{q}_j^{n+\frac{1}{2}} \approx \tilde{\boldsymbol{q}}^n(x_j) + \frac{\Delta t}{2}\,\boldsymbol{q}_t(x_j, t^n)$$

- $\tilde{\boldsymbol{q}}^n(x) = \bar{\boldsymbol{q}}_j^n + (\boldsymbol{q}_x)_j^n(x - x_j) \Longrightarrow \boxed{\tilde{\boldsymbol{q}}^n(x_j) = \bar{\boldsymbol{q}}_j^n}$

- $\boxed{\boldsymbol{q}_t(x_j, t^n) = -\boldsymbol{f}(\bar{\boldsymbol{q}}_j^n)_x}$

The space derivatives $\boldsymbol{f}_x$ are computed using the (minmod) limiter:

$$\boldsymbol{f}(\bar{\boldsymbol{q}}_j^n)_x = \text{minmod}\left(\theta\,\frac{\boldsymbol{f}(\bar{\boldsymbol{q}}_j^n) - \boldsymbol{f}(\bar{\boldsymbol{q}}_{j-1}^n)}{\Delta x}, \frac{\boldsymbol{f}(\bar{\boldsymbol{q}}_{j+1}^n) - \boldsymbol{f}(\bar{\boldsymbol{q}}_{j-1}^n)}{2\Delta x}, \theta\,\frac{\boldsymbol{f}(\bar{\boldsymbol{q}}_{j+1}^n) - \boldsymbol{f}(\bar{\boldsymbol{q}}_j^n)}{\Delta x}\right)$$

Higher-Order and Multidimensional Staggered Central Schemes

[Arminjon, Viallon, Madrane; 1997]

[Jiang, Tadmor; 1998]

[Liu, Tadmor; 1998]

[Bianco, Puppo, Russo; 1999]

[Levy, Puppo, Russo; 1999, 2000, 2002]

[Lie, Noelle; 2000]

Central-Upwind Schemes

Goal: **to reduce numerical dissipation of central schemes**

Example — Numerical Dissipation of the Staggered LxF Scheme

$$q^{n+1}_{j+\frac{1}{2}} = \frac{q^n_{j+1} + q^n_j}{2} - \frac{\Delta t}{\Delta x}\left[f(q^n_{j+1}) - f(q^n_j)\right]$$

$$q^{n+1}_{j+\frac{1}{2}} - q^n_{j+\frac{1}{2}} + \frac{\Delta t}{\Delta x}\left[f(q^n_{j+1}) - f(q^n_j)\right] = \frac{q^n_{j+1} - 2q^n_{j+\frac{1}{2}} + q^n_j}{2}$$

$$\frac{q^{n+1}_{j+\frac{1}{2}} - q^n_{j+\frac{1}{2}}}{\Delta t} + \frac{f(q^n_{j+1}) - f(q^n_j)}{\Delta x} = \boxed{\frac{(\Delta x)^2}{8\Delta t}} \cdot \frac{q^n_{j+1} - 2q^n_{j+\frac{1}{2}} + q^n_j}{(\Delta x/2)^2}$$

- As Δt decreases, the numerical dissipation increases
- As $\Delta t \sim (\Delta x)^2$, the LxF scheme is inconsistent
- As $\Delta t \to 0$, the numerical dissipation blows up

Central-Upwind Schemes

- Godunov-type finite-volume methods

- Central: Riemann-problem-solver-free methods designed without tracking complicated nonlinear waves

- Upwind: Use some information on wave propagation to reduce numerical dissipation and thus enhance the resolution of nonsmooth waves

- Can be applied as a "black-box" solver to hyperbolic (systems of) PDEs

- Robust, efficient and highly accurate

Selected Scientific Applications

- Gas dynamics and granular hydrodynamics
- Compressible multi-fluid and multi-phase flows
- Dusty gas flows
- Shallow water equations and related models
- Propagation of pollutant models
- Traffic and pedestrian flow models
- Incompressible Navier-Stokes equations
- Buckley-Leverett equation and polymer systems
- Glacier growth models
- Combustion and stiff detonation waves
- Chemotaxis and haptotaxis models
- Elastic waves in heterogeneous media
- Optimal control problems governed by nonlinear hyperbolic PDEs

Some Industrial Application

• Central-upwind schemes have been implemented in the industrial open source CFD software package OpenFOAM

[Gasparini, Greenshields, Weller; 2008]

OpenCFD Ltd – `http://www.opencfd.co.uk`

3-D, polyhedral meshes with collocated variables, complex geometry, complex physics

Widely used in industry, consultancy and academia worldwide including the European Space Agency (ESA)

• Central-upwind schemes have been implemented at the National Center of Computational Hydroscience and Engineering at the University of Mississippi, where they became the core part of the GIS-based decision support systems for flood mitigation and management.

These systems are currently being used by several US federal agencies

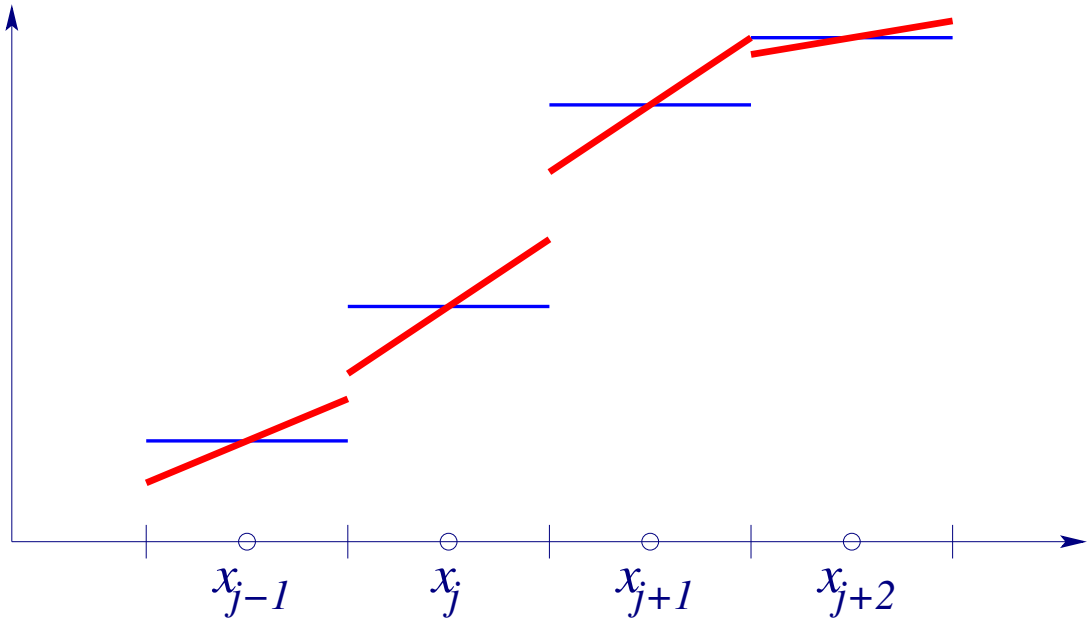

$$\tilde{\boldsymbol{q}}^n(x) = \bar{\boldsymbol{q}}_j^n + (\boldsymbol{q}_x)_j^n (x - x_j) \quad \text{for } x \in C_j$$

$$\boldsymbol{q}^-_{j+\frac{1}{2}} := \lim_{x \to x_{j+\frac{1}{2}}-} \tilde{\boldsymbol{q}}(x, t^n) = \bar{\boldsymbol{q}}_j^n + \frac{\Delta x}{2} (\boldsymbol{q}_x)_j^n$$

$$\boldsymbol{q}^+_{j+\frac{1}{2}} := \lim_{x \to x_{j+\frac{1}{2}}+} \tilde{\boldsymbol{q}}(x, t^n) = \bar{\boldsymbol{q}}_{j+1}^n - \frac{\Delta x}{2} (\boldsymbol{q}_x)_{j+1}^n$$

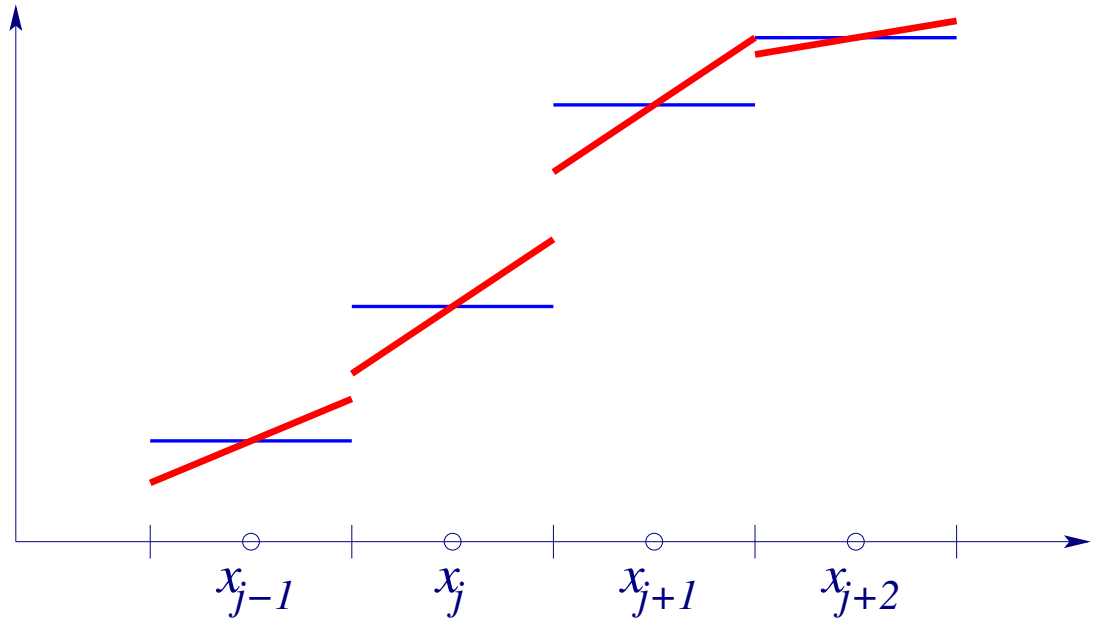

The discontinuities appearing at the reconstruction step at the interface points $\{x_{j+\frac{1}{2}}\}$ propagate at finite speeds estimated by:

$$a^+_{j+\frac{1}{2}} := \max\left\{\lambda_N\left(\frac{\partial \boldsymbol{f}}{\partial \boldsymbol{q}}(\boldsymbol{q}^-_{j+\frac{1}{2}})\right), \lambda_N\left(\frac{\partial \boldsymbol{f}}{\partial \boldsymbol{q}}(\boldsymbol{q}^+_{j+\frac{1}{2}})\right), 0\right\}$$

$$a^-_{j+\frac{1}{2}} := \min\left\{\lambda_1\left(\frac{\partial \boldsymbol{f}}{\partial \boldsymbol{q}}(\boldsymbol{q}^-_{j+\frac{1}{2}})\right), \lambda_1\left(\frac{\partial \boldsymbol{f}}{\partial \boldsymbol{q}}(\boldsymbol{q}^+_{j+\frac{1}{2}})\right), 0\right\}$$

$\lambda_1 < \lambda_2 < \ldots < \lambda_N$: N eigenvalues of the Jacobian $\frac{\partial \boldsymbol{f}}{\partial \boldsymbol{q}}$

Idea: **Select control volumes according to the size of each Riemann fan**

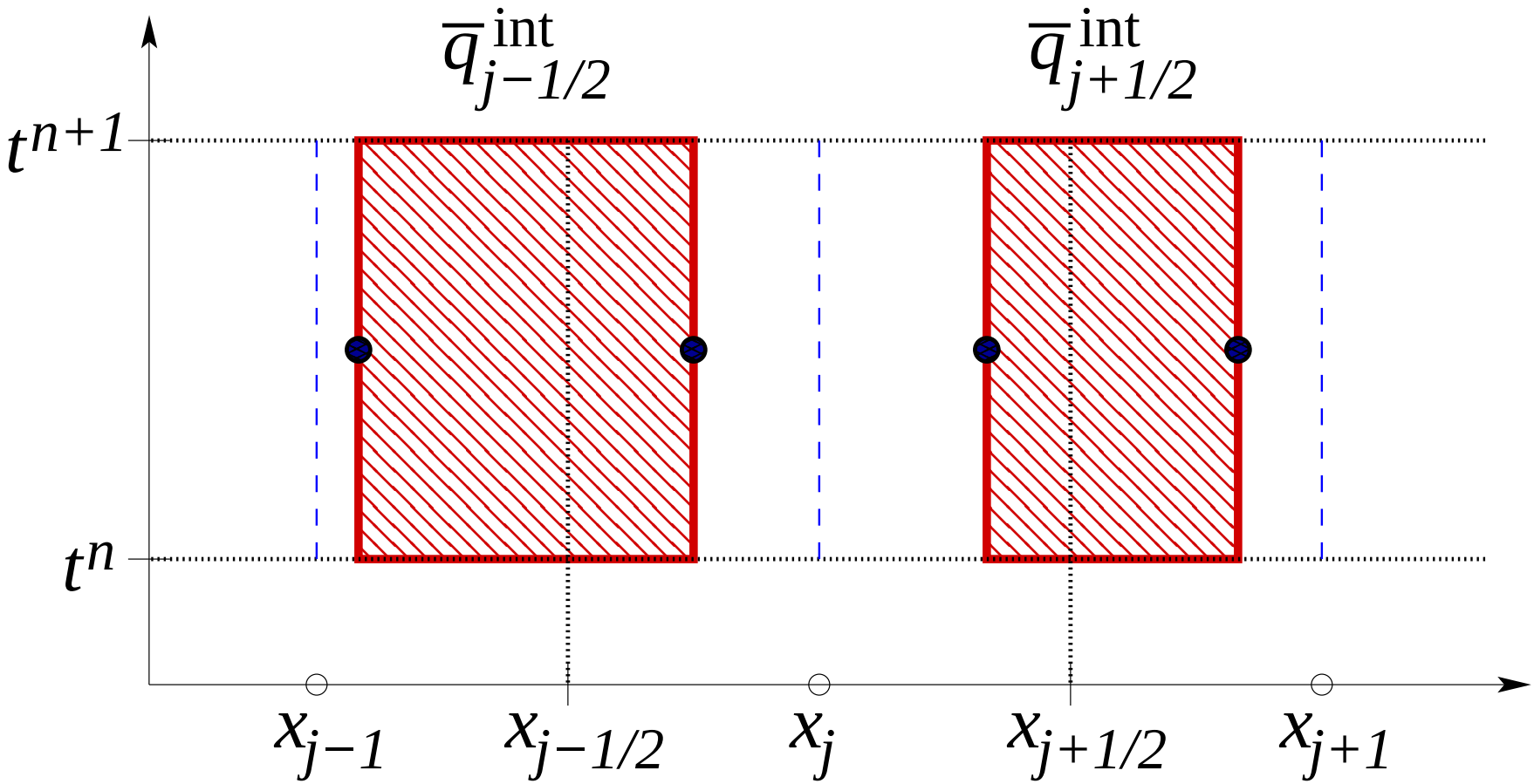

$$\left[x_{j-\frac{1}{2}} + a^{-}_{j-\frac{1}{2}}\Delta t, x_{j-\frac{1}{2}} + a^{+}_{j-\frac{1}{2}}\Delta t\right] \times [t^{n}, t^{n+1}]$$

$$\left[x_{j+\frac{1}{2}} + a^{-}_{j+\frac{1}{2}}\Delta t, x_{j+\frac{1}{2}} + a^{+}_{j+\frac{1}{2}}\Delta t\right] \times [t^{n}, t^{n+1}]$$

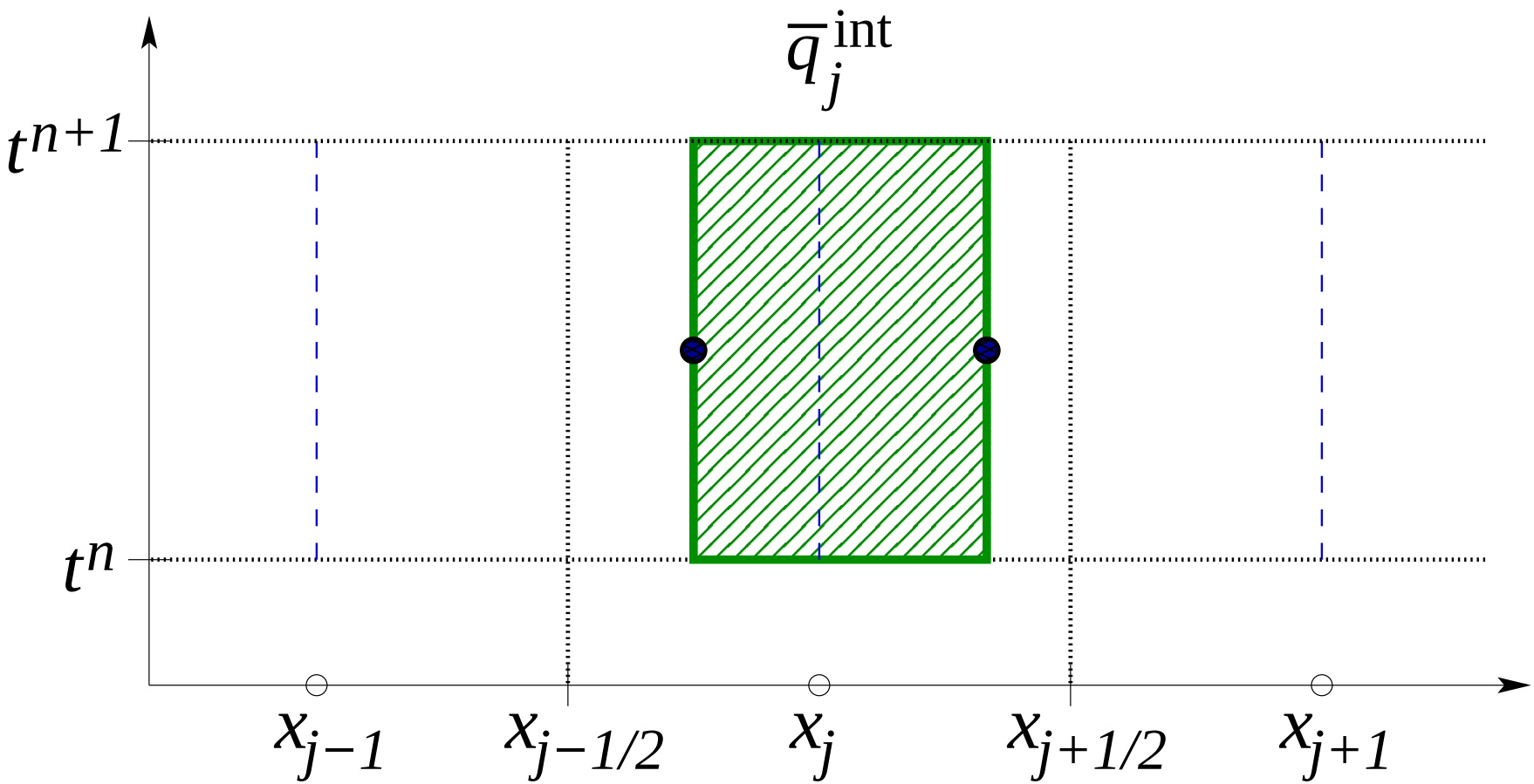

$$\left[x_{j-\frac{1}{2}} + a^+_{j-\frac{1}{2}}\Delta t, x_{j+\frac{1}{2}} + a^-_{j-\frac{1}{2}}\Delta t\right] \times [t^n, t^{n+1}]$$

Final Step: **Projection onto the Original Grid**

A piecewise linear interpolant, $\tilde{\boldsymbol{q}}^{\text{int}}(x)$, reconstructed from the evolved intermediate cell averages $\{\bar{\boldsymbol{q}}_j^{\text{int}}\}$ and $\{\bar{\boldsymbol{q}}_{j+\frac{1}{2}}^{\text{int}}\}$, is projected back onto the original grid by averaging it over the intervals $[x_{j-\frac{1}{2}}, x_{j+\frac{1}{2}}]$.

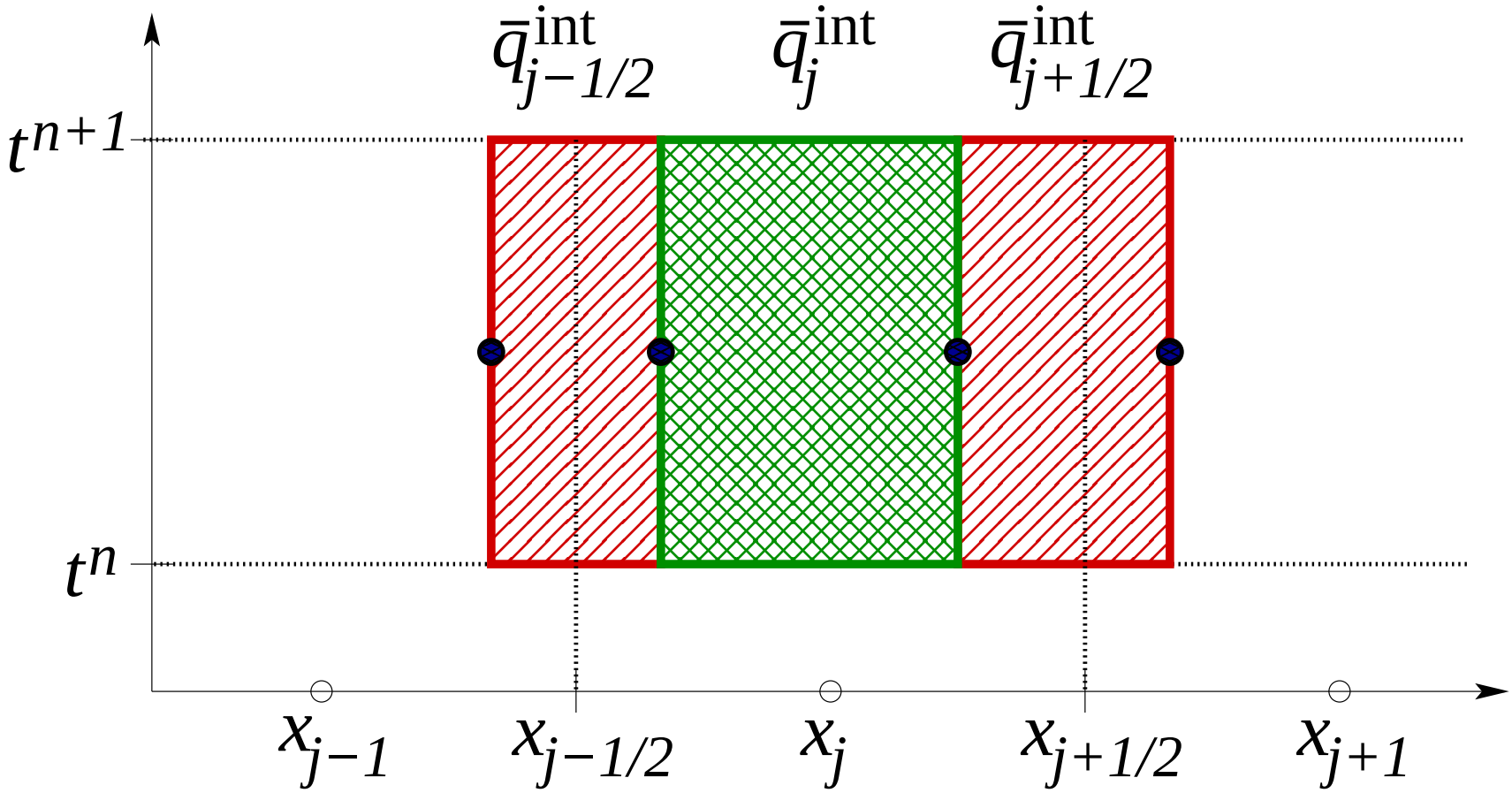

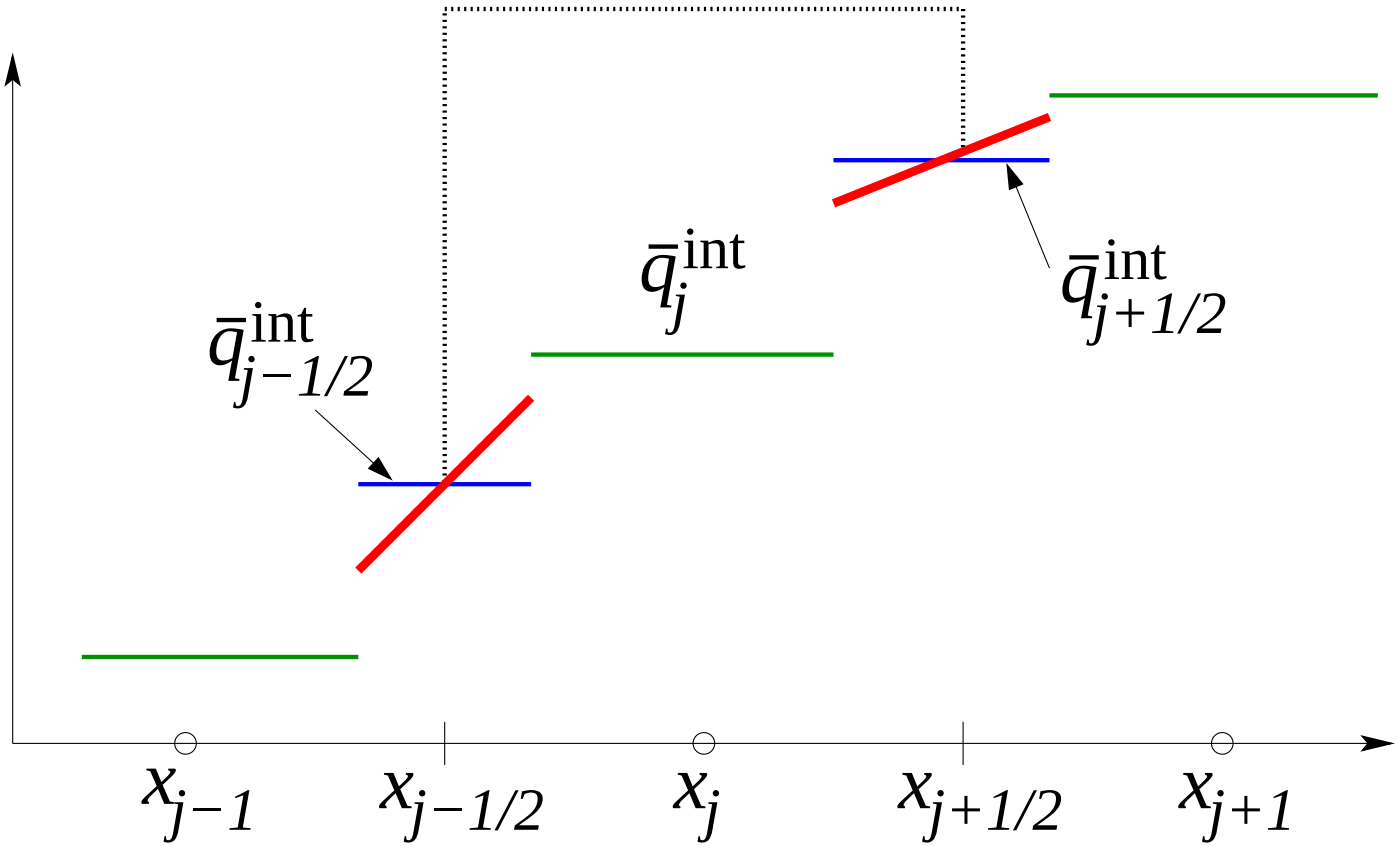

New projected cell averages:

$$\bar{\boldsymbol{q}}_j^{n+1} = \frac{a^+_{j-\frac{1}{2}}\Delta t}{\Delta x}\bar{\boldsymbol{q}}^{\text{int}}_{j-\frac{1}{2}} + \left[1 + \frac{\left(a^-_{j-\frac{1}{2}} - a^+_{j+\frac{1}{2}}\right)\Delta t}{\Delta x}\right]\bar{\boldsymbol{q}}^{\text{int}}_j - \frac{a^-_{j+\frac{1}{2}}\Delta t}{\Delta x}\bar{\boldsymbol{q}}^{\text{int}}_{j+\frac{1}{2}}$$
$$+\frac{(\Delta t)^2}{2\Delta x}\left[\boxed{(\boldsymbol{q}_x)^{\text{int}}_{j+\frac{1}{2}}}\,a^+_{j+\frac{1}{2}}a^-_{j+\frac{1}{2}} - \boxed{(\boldsymbol{q}_x)^{\text{int}}_{j-\frac{1}{2}}}\,a^+_{j-\frac{1}{2}}a^-_{j-\frac{1}{2}}\right]$$

1-D Semi-Discrete Central-Upwind Scheme

$$\frac{d}{dt}\bar{\boldsymbol{q}}_j(t^n) = \lim_{\Delta t\to 0}\frac{\bar{\boldsymbol{q}}_j^{n+1}-\bar{\boldsymbol{q}}_j^{n}}{\Delta t} = \frac{a^+_{j-\frac{1}{2}}}{\Delta x}\lim_{\Delta t\to 0}\bar{\boldsymbol{q}}^{\text{int}}_{j-\frac{1}{2}} - \frac{a^-_{j+\frac{1}{2}}}{\Delta x}\lim_{\Delta t\to 0}\bar{\boldsymbol{q}}^{\text{int}}_{j+\frac{1}{2}}$$
$$+\frac{a^-_{j-\frac{1}{2}}-a^+_{j+\frac{1}{2}}}{\Delta x}\lim_{\Delta t\to 0}\bar{\boldsymbol{q}}^{\text{int}}_{j} + \lim_{\Delta t\to 0}\left\{\frac{\bar{\boldsymbol{q}}^{\text{int}}_j-\bar{\boldsymbol{q}}^{n}_j}{\Delta t}\right\}$$
$$+\frac{1}{2\Delta x}\lim_{\Delta t\to 0}\left[\Delta t\left((\boldsymbol{q}_x)^{\text{int}}_{j+\frac{1}{2}}a^+_{j+\frac{1}{2}}a^-_{j+\frac{1}{2}} - (\boldsymbol{q}_x)^{\text{int}}_{j-\frac{1}{2}}a^+_{j-\frac{1}{2}}a^-_{j-\frac{1}{2}}\right)\right]$$

We then substitute $\boldsymbol{q}^{\text{int}}_{j\pm\frac{1}{2}}$, $\boldsymbol{q}^{\text{int}}_j$ and $(\boldsymbol{q}_x)^{\text{int}}_{j\pm\frac{1}{2}}$ into here to obtain the 1-D semi-discrete central-upwind scheme

(for details see [Kurganov, Lin; 2007])

$$\frac{d}{dt}\bar{\boldsymbol{q}}_j(t) = -\frac{\boldsymbol{H}_{j+\frac{1}{2}}(t) - \boldsymbol{H}_{j-\frac{1}{2}}(t)}{\Delta x}$$

The central-upwind numerical flux is:

$$\boldsymbol{H}_{j+\frac{1}{2}} = \frac{a^+_{j+\frac{1}{2}}\boldsymbol{f}(\boldsymbol{q}^-_{j+\frac{1}{2}}) - a^-_{j+\frac{1}{2}}\boldsymbol{f}(\boldsymbol{q}^+_{j+\frac{1}{2}})}{a^+_{j+\frac{1}{2}} - a^-_{j+\frac{1}{2}}} + a^+_{j+\frac{1}{2}}a^-_{j+\frac{1}{2}}\left[\frac{\boldsymbol{q}^+_{j+\frac{1}{2}} - \boldsymbol{q}^-_{j+\frac{1}{2}}}{a^+_{j+\frac{1}{2}} - a^-_{j+\frac{1}{2}}} - \boxed{\boldsymbol{d}_{j+\frac{1}{2}}}\right]$$

The built-in "anti-diffusion" term is:

$$\boldsymbol{d}_{j+\frac{1}{2}} = \frac{1}{2}\lim_{\Delta t\to 0}\left\{\Delta t(\boldsymbol{q}_x)^{\text{int}}_{j+\frac{1}{2}}\right\} = \text{minmod}\left(\frac{\boldsymbol{q}^+_{j+\frac{1}{2}} - \boldsymbol{q}^*_{j+\frac{1}{2}}}{a^+_{j+\frac{1}{2}} - a^-_{j+\frac{1}{2}}}, \frac{\boldsymbol{q}^*_{j+\frac{1}{2}} - \boldsymbol{q}^-_{j+\frac{1}{2}}}{a^+_{j+\frac{1}{2}} - a^-_{j+\frac{1}{2}}}\right)$$

The intermediate values $\boldsymbol{q}^*_{j+\frac{1}{2}}$ are:

$$\boldsymbol{q}^*_{j+\frac{1}{2}} = \lim_{\Delta t\to 0}\bar{\boldsymbol{q}}^{\text{int}}_{j+\frac{1}{2}} = \frac{a^+_{j+\frac{1}{2}}\boldsymbol{q}^+_{j+\frac{1}{2}} - a^-_{j+\frac{1}{2}}\boldsymbol{q}^-_{j+\frac{1}{2}} - \left\{\boldsymbol{f}(\boldsymbol{q}^+_{j+\frac{1}{2}}) - \boldsymbol{f}(\boldsymbol{q}^-_{j+\frac{1}{2}})\right\}}{a^+_{j+\frac{1}{2}} - a^-_{j+\frac{1}{2}}}$$

Remarks

1. $\boldsymbol{d}_{j+\frac{1}{2}} \equiv 0$ corresponds to the central-upwind scheme from [Kurganov, Noelle, Petrova; 2001]

2. $\boldsymbol{d}_{j+\frac{1}{2}} \equiv 0$ and $a^{+}_{j+\frac{1}{2}} \equiv -a^{-}_{j+\frac{1}{2}}$ correspond to the original scheme from [Kurganov, Tadmor; 2000]

3. The (formal) order of the scheme is determined only by the order of the piecewise polynomial reconstruction $\widetilde{\boldsymbol{q}}$, used to compute the values $\boldsymbol{q}^{\pm}_{j+\frac{1}{2}}$, and the order of the ODE solver

4. Recommended ODE solver for nonlinear hyperbolic problems is the 3-stage third-order strong stability preserving (SSP) Runge-Kutta method

[Shu, Osher; 1988, 1989]

[Gottlieb, Shu, Tadmor; 2001]

[Gottlieb, Ketcheson, Shu; 2011]

Central schemes have been successfully extended to more complicated problems arising in a wide variety of applications:

- Convection-diffusion equations $\boldsymbol{q}_t + \boldsymbol{f}(\boldsymbol{q})_x = \nu \boldsymbol{q}_{xx}$

Chertock, Kurganov, Levy, Petrova, Tadmor, ...

- Balance laws $\boldsymbol{q}_t + \boldsymbol{f}(\boldsymbol{q})_x = \boldsymbol{S}(\boldsymbol{q})$

Castro, Chertock, Kurganov, Levy, Morales de Luna, Noelle, Pareschi, Petrova, Russo, ...

- Nonconservative hyperbolic systems $\boldsymbol{q}_t + \boldsymbol{f}(\boldsymbol{q})_x = B(\boldsymbol{q})\boldsymbol{q}_x$

Castro, Cheng, Chertock, Karni, Kirr, Kurganov, Petrova, ...

1-D Gas Dynamics

$$\frac{\partial}{\partial t}\begin{bmatrix} \rho \\ \rho u \\ E \end{bmatrix} + \frac{\partial}{\partial x}\begin{bmatrix} \rho u \\ \rho u^2 + p \\ u(E+p) \end{bmatrix} = 0$$

$p = (\gamma - 1)\left[E - \frac{\rho u^2}{2}\right]$: equation of state

ρ: density

u: velocity

p: pressure

E: total energy

$\gamma = 1.4$

Example — Moving Contact Wave

Initial data:

$$(\rho, u, p)(x, 0) = \begin{cases} (1.4, 0.1, 1), & x < 0.5 \\ (1.0, 0.1, 1), & x > 0.5 \end{cases}$$

Final time: $t = 2$

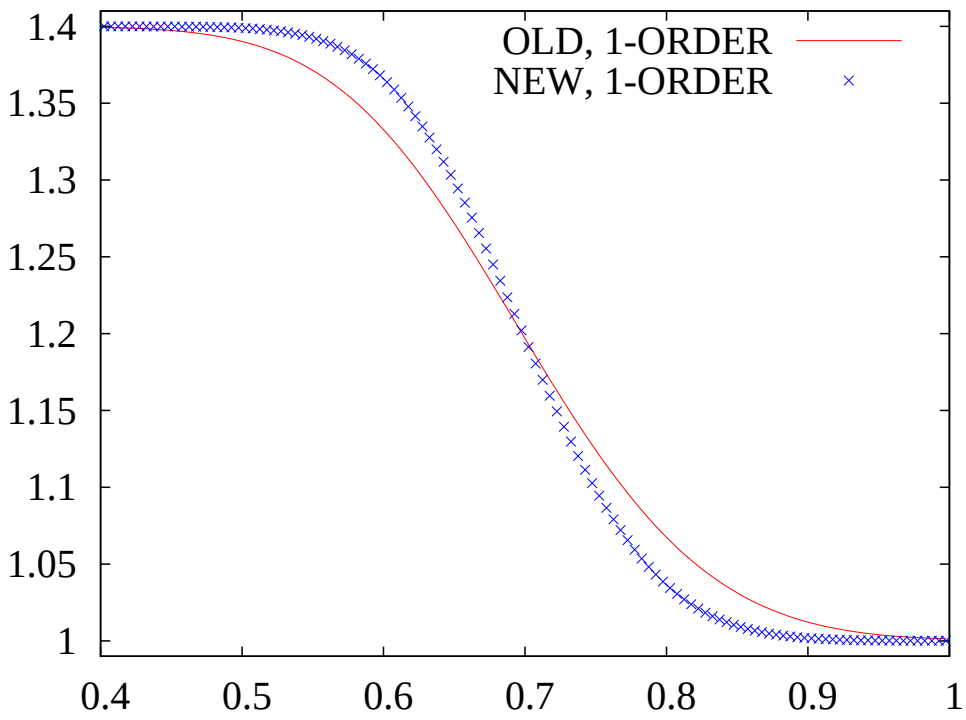

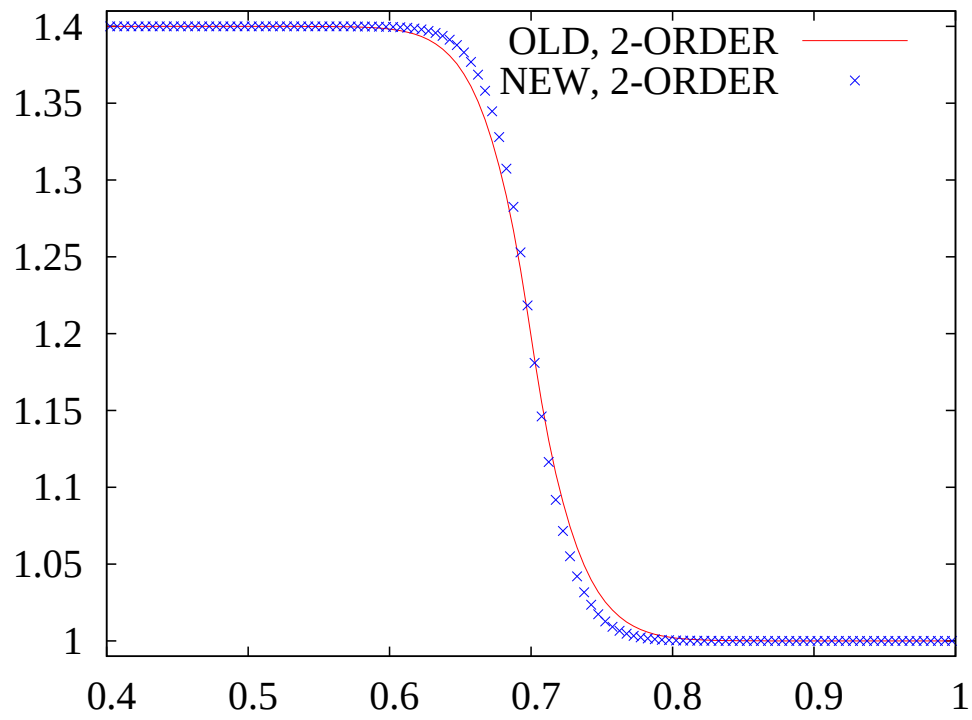

Example — Stationary Contact Wave and Traveling Shock and Rarefaction

Initial data:

$$(\rho, u, p)(x, 0) = \begin{cases} (1, -19.59745, 1000), & x < 0.8 \\ (1, -19.59745, 0.01), & x > 0.8 \end{cases}$$

Final time: $t = 0.012$

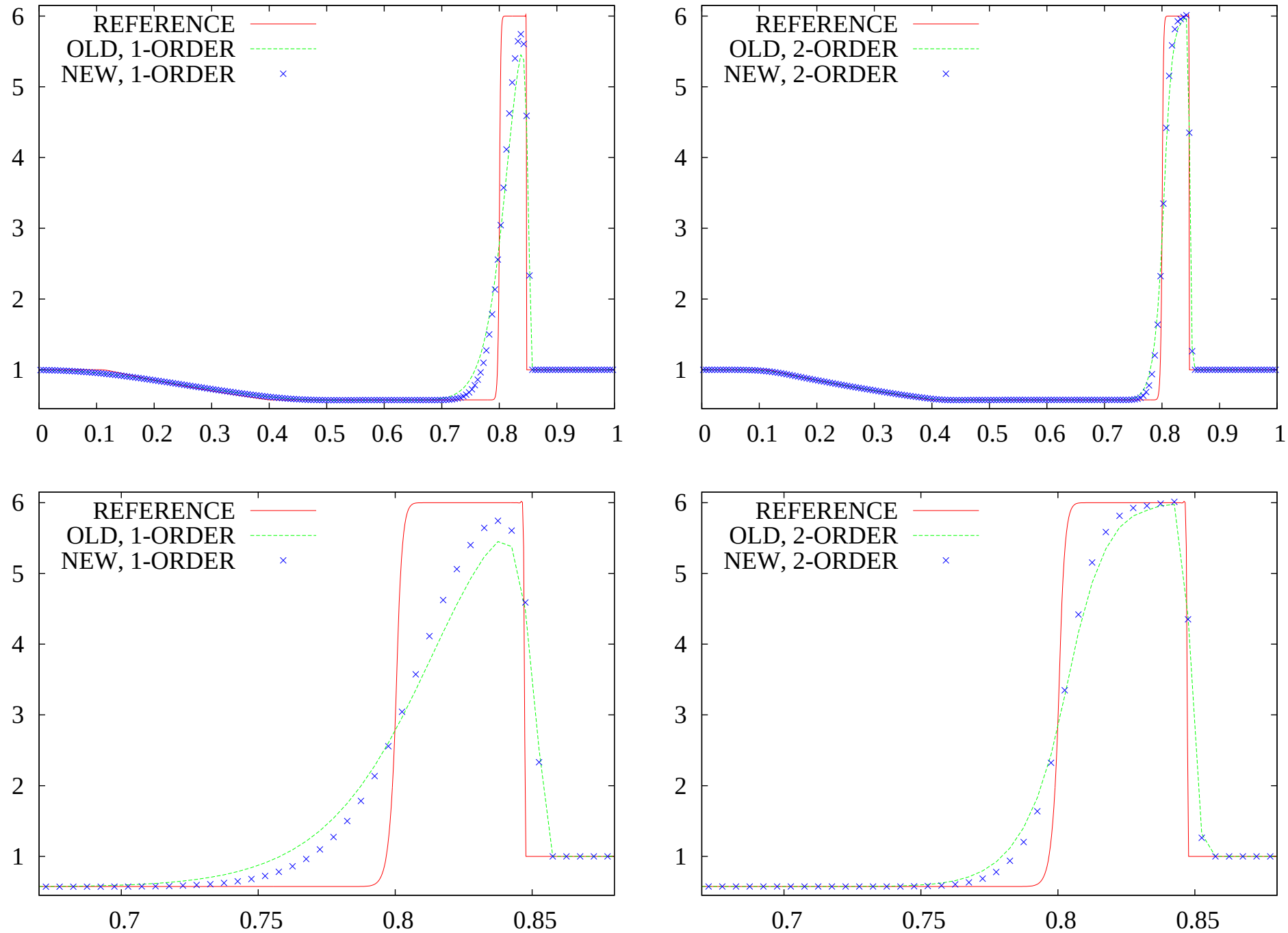
REFERENCE
OLD, 1-ORDER
NEW, 1-ORDER
REFERENCE
OLD, 2-ORDER
NEW, 2-ORDER
REFERENCE
OLD, 1-ORDER
NEW, 1-ORDER
REFERENCE
OLD, 2-ORDER
NEW, 2-ORDER
1
2
3
4
5
6
0
0.1
0.2
0.3
0.4
0.5
0.6
0.7
0.8
0.9
1
0.7
0.75
0.8
0.85

2-D Finite-Volume Methods

$$\boldsymbol{q}_t + \boldsymbol{f}(\boldsymbol{q})_x + \boldsymbol{g}(\boldsymbol{q})_y = \boldsymbol{0}$$

Consider Cartesian cells $C_{j,k} := [x_{j-\frac{1}{2}}, x_{j+\frac{1}{2}}] \times [y_{k-\frac{1}{2}}, y_{k+\frac{1}{2}}]$ centered at $x_j := j\Delta x$, $y_k := k\Delta y$.

Consider a uniform grid in time with the time levels $t^n := n\Delta t$.

$$\bar{\boldsymbol{q}}_{j,k}^n \approx \frac{1}{\Delta x \Delta y} \iint_{C_{j,k}} \boldsymbol{q}(x, y, t^n)\, dy\, dx : \text{ cell averages}$$

These cell averages are then evolved to the next time level $t = t^{n+1}$ in three consecutive steps: reconstruction, evolution and projection.

Reconstruction

Second-order piecewise linear interpolant:

$$\tilde{\boldsymbol{q}}(x,y,t^n) = \sum_{j,k} \left[\bar{\boldsymbol{q}}^n_{j,k} + (\boldsymbol{q}_x)^n_{j,k}(x - x_j) + (\boldsymbol{q}_y)^n_{j,k}(y - y_k) \right] \chi_{j,k}(x,y)$$

$\chi_{j,k}(x,y)$: the characteristic function of the interval $C_{j,k}$

$$(\boldsymbol{q}_x)^n_{j,k} \approx \boldsymbol{q}_x(x_j, y_k, t^n), \qquad (\boldsymbol{q}_y)^n_{j,k} \approx \boldsymbol{q}_y(x_j, y_k, t^n)$$

$$\boxed{\begin{aligned} (\boldsymbol{q}_x)^n_{j,k} &= \text{minmod}\left(\theta \frac{\bar{\boldsymbol{q}}^n_{j+1,k} - \bar{\boldsymbol{q}}^n_{j,k}}{\Delta x}, \frac{\bar{\boldsymbol{q}}^n_{j+1,k} - \bar{\boldsymbol{q}}^n_{j-1,k}}{2\Delta x}, \theta \frac{\bar{\boldsymbol{q}}^n_{j,k} - \bar{\boldsymbol{q}}^n_{j-1,k}}{\Delta x} \right) \\ (\boldsymbol{q}_y)^n_{j,k} &= \text{minmod}\left(\theta \frac{\bar{\boldsymbol{q}}^n_{j,k+1} - \bar{\boldsymbol{q}}^n_{j,k}}{\Delta y}, \frac{\bar{\boldsymbol{q}}^n_{j,k+1} - \bar{\boldsymbol{q}}^n_{j,k-1}}{2\Delta y}, \theta \frac{\bar{\boldsymbol{q}}^n_{j,k} - \bar{\boldsymbol{q}}^n_{j,k-1}}{\Delta y} \right) \end{aligned}}$$

$\theta \in [1, 2]$

Reconstructed Point Values

$$\boldsymbol{q}^{\mathsf{N}}_{j,k} := \bar{\boldsymbol{q}}^{n}_{j,k} + \frac{\Delta y}{2}(\boldsymbol{q}_y)^{n}_{j,k}$$

$$\boldsymbol{q}^{\mathsf{W}}_{j,k} := \bar{\boldsymbol{q}}^{n}_{j,k} - \frac{\Delta x}{2}(\boldsymbol{q}_x)^{n}_{j,k}$$

$$\boldsymbol{q}^{\mathsf{E}}_{j,k} := \bar{\boldsymbol{q}}^{n}_{j,k} + \frac{\Delta x}{2}(\boldsymbol{q}_x)^{n}_{j,k}$$

$$\boldsymbol{q}^{\mathsf{S}}_{j,k} := \bar{\boldsymbol{q}}^{n}_{j,k} - \frac{\Delta y}{2}(\boldsymbol{q}_y)^{n}_{j,k}$$

Evolution

Consider a general quadrilateral

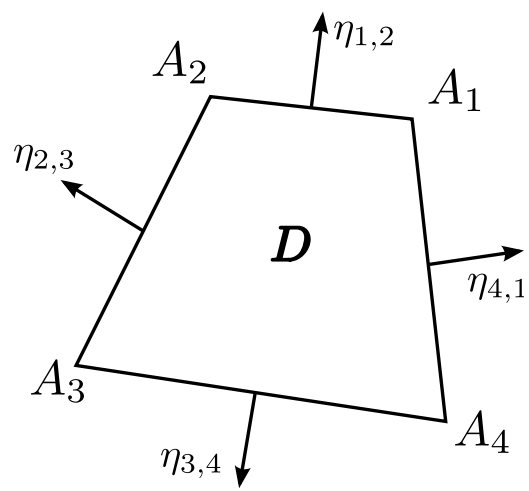

$$\bar{\boldsymbol{q}}_D^{n+1} = \frac{1}{|D|} \iint_D \tilde{\boldsymbol{q}}(x, y, t^n)\, dx\, dy - \frac{1}{|D|} \int_{t^n}^{t^{n+1}} \oint_{\partial D} [\eta^x \boldsymbol{f}(\boldsymbol{q}) + \eta^y \boldsymbol{g}(\boldsymbol{q})]\, ds\, dt$$

$\boldsymbol{\eta} = (\eta^x, \eta^y)^T$: outer unit normal vector to ∂D

2-D upwinding is quite problematic even for 1-order schemes on Cartesian grid!

Easy (robust, accurate, efficient) alternatives: staggered central and central-upwind schemes

Multidimensional Staggered Central Schemes:

[Arminjon, Viallon, Madrane; 1997]

[Jiang, Tadmor; 1998]

[Levy, Puppo, Russo; 1999, 2000, 2002]

[Lie, Noelle; 2000]

2-D Central-Upwind Schemes

[Kurganov, Prugger, Wu; 2017]

Consider a Cartesian cell $C_{j,k}$.

The one-sided local speeds at the midpoint of the cell edges can be estimated by

$$
\begin{aligned}
a^{+}_{j+\frac{1}{2},k} &:= \max\left\{\lambda_N\left(\frac{\partial \boldsymbol{f}}{\partial \boldsymbol{q}}\left(\boldsymbol{q}^{\mathsf{W}}_{j+1,k}\right)\right), \lambda_N\left(\frac{\partial \boldsymbol{f}}{\partial \boldsymbol{q}}\left(\boldsymbol{q}^{\mathsf{E}}_{j,k}\right)\right), 0\right\}\\
a^{-}_{j+\frac{1}{2},k} &:= \min\left\{\lambda_1\left(\frac{\partial \boldsymbol{f}}{\partial \boldsymbol{q}}\left(\boldsymbol{q}^{\mathsf{W}}_{j+1,k}\right)\right), \lambda_1\left(\frac{\partial \boldsymbol{f}}{\partial \boldsymbol{q}}\left(\boldsymbol{q}^{\mathsf{E}}_{j,k}\right)\right), 0\right\}\\
b^{+}_{j,k+\frac{1}{2}} &:= \max\left\{\lambda_N\left(\frac{\partial \boldsymbol{g}}{\partial \boldsymbol{q}}\left(\boldsymbol{q}^{\mathsf{S}}_{j,k+1}\right)\right), \lambda_N\left(\frac{\partial \boldsymbol{g}}{\partial \boldsymbol{q}}\left(\boldsymbol{q}^{\mathsf{N}}_{j,k}\right)\right), 0\right\}\\
b^{-}_{j,k+\frac{1}{2}} &:= \min\left\{\lambda_1\left(\frac{\partial \boldsymbol{g}}{\partial \boldsymbol{q}}\left(\boldsymbol{q}^{\mathsf{S}}_{j,k+1}\right)\right), \lambda_1\left(\frac{\partial \boldsymbol{g}}{\partial \boldsymbol{q}}\left(\boldsymbol{q}^{\mathsf{N}}_{j,k}\right)\right), 0\right\}
\end{aligned}
$$

$\lambda_1 < \lambda_2 < \ldots < \lambda_N$: eigenvalues of the Jacobians $\partial \boldsymbol{f}/\partial \boldsymbol{q}$ and $\partial \boldsymbol{g}/\partial \boldsymbol{q}$

Using the one-sided speed bounds, we split the computational domain $\bigcup C_{j,k}$ into the nonsymmetric subdomains:

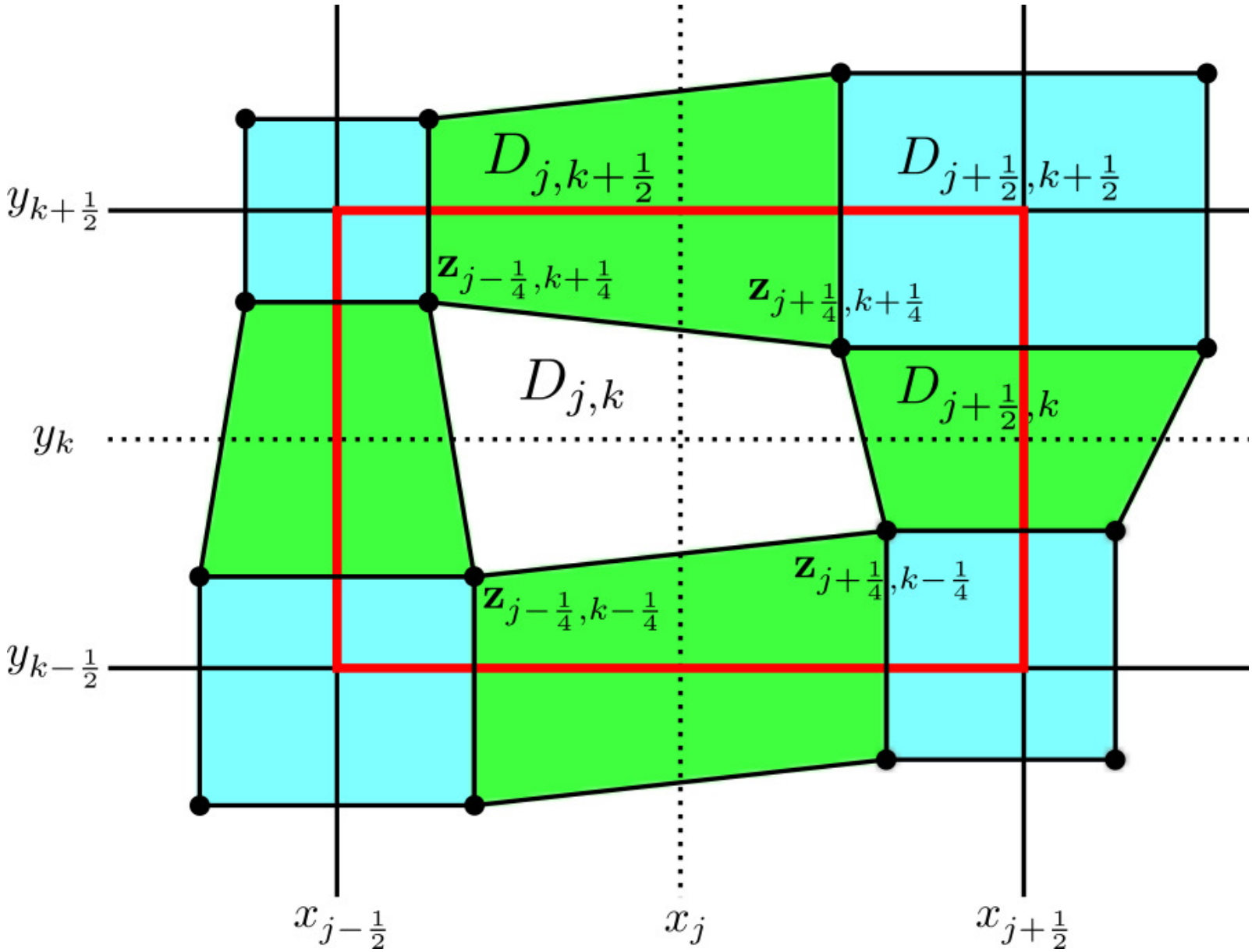

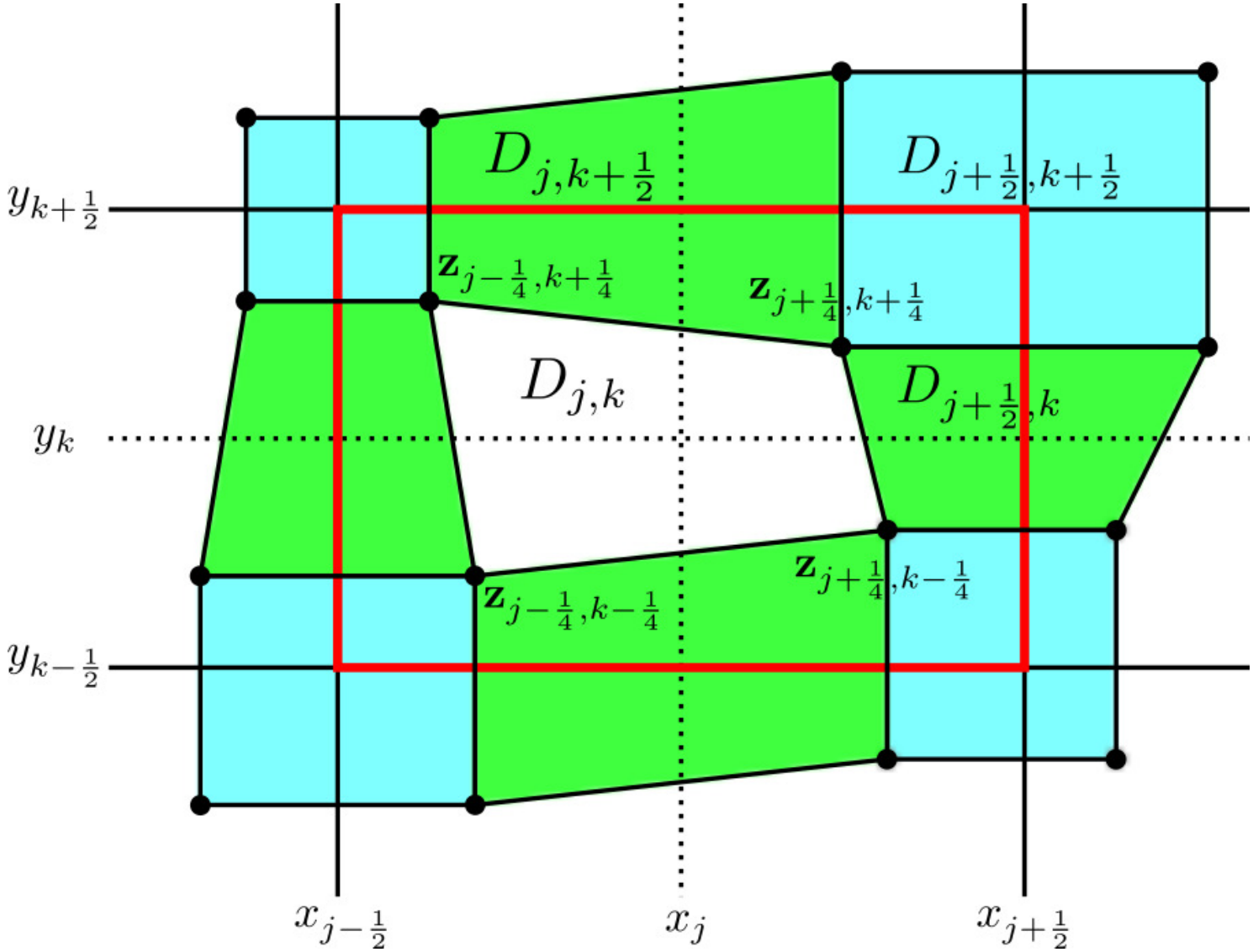

Thanks to the finite speed of propagation, the evolved solution will remain smooth in the central subdomains $D_{j,k}$ for all $t \in [t^n, t^{n+1})$.

Central Nessyahu-Tadmor-Type Evolution

Recall

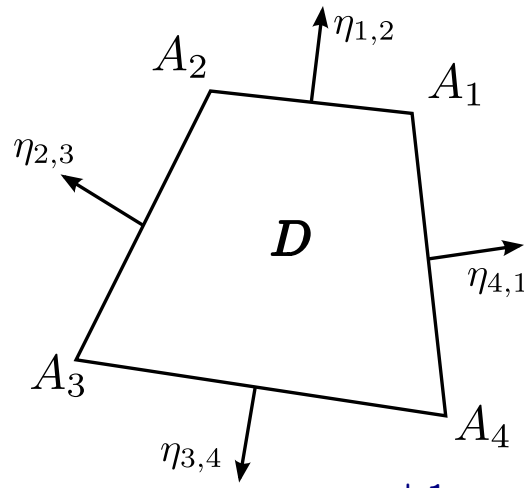

$$\bar{\boldsymbol{q}}_D^{\text{int}} = \frac{1}{|D|} \iint_D \tilde{\boldsymbol{q}}(x, y, t^n)\, dx\, dy - \frac{1}{|D|} \int_{t^n}^{t^{n+1}} \oint_{\partial D} [\eta^x \boldsymbol{f}(\boldsymbol{q}) + \eta^y \boldsymbol{g}(\boldsymbol{q})]\, ds\, dt$$

$$\boldsymbol{H}_{12} := \int_{t^n}^{t^{n+1}} \int_{A_1}^{A_2} \left[\eta_{12}^x \boldsymbol{f}(\boldsymbol{q}) + \eta_{12}^y \boldsymbol{g}(\boldsymbol{q})\right] ds\, dt$$

$$\approx \frac{\Delta t\, |A_1 A_2|}{2} \Big[\eta_{12}^x \Big(\boldsymbol{f}\big(\boldsymbol{q}(A_1, t^{n+\frac{1}{2}})\big) + \boldsymbol{f}\big(\boldsymbol{q}(A_2, t^{n+\frac{1}{2}})\big)\Big)$$

$$+ \eta_{12}^y \Big(\boldsymbol{g}\big(\boldsymbol{q}(A_1, t^{n+\frac{1}{2}})\big) + \boldsymbol{g}\big(\boldsymbol{q}(A_2, t^{n+\frac{1}{2}})\big)\Big)\Big]$$

The solution at the points A_i, $i = 1, 2, 3, 4$ is smooth for $t \in [t^n, t^{n+1})$.

The midpoint values are obtained using the Taylor expansion in time:

$$\boldsymbol{q}(A_i, t^{n+\frac{1}{2}}) = \boldsymbol{q}(A_i, t^n) - \frac{\Delta t}{2}\left[\boldsymbol{f}(\boldsymbol{q}(A_i, t^n))_x + \boldsymbol{g}(\boldsymbol{q}(A_i, t^n))_y\right] + \mathcal{O}((\Delta t)^2)$$

$$\approx \tilde{\boldsymbol{q}}(A_i, t^n) - \frac{\Delta t}{2}\left[(\boldsymbol{f}(\boldsymbol{q})_x)^n_{A_i} + (\boldsymbol{g}(\boldsymbol{q})_y)^n_{A_i}\right]$$

$$(\boldsymbol{f}(\boldsymbol{q})_x)^n_{A_i} = \text{minmod}\left(\frac{\boldsymbol{f}(\bar{\boldsymbol{q}}^n_{j+1,k}) - \boldsymbol{f}(\bar{\boldsymbol{q}}^n_{j,k})}{\Delta x}, \frac{\boldsymbol{f}(\bar{\boldsymbol{q}}^n_{j,k}) - \boldsymbol{f}(\bar{\boldsymbol{q}}^n_{j-1,k})}{\Delta x}\right)$$

$$(\boldsymbol{g}(\boldsymbol{q})_y)^n_{A_i} = \text{minmod}\left(\frac{\boldsymbol{g}(\bar{\boldsymbol{q}}^n_{j,k+1}) - \boldsymbol{g}(\bar{\boldsymbol{q}}^n_{j,k})}{\Delta y}, \frac{\boldsymbol{g}(\bar{\boldsymbol{q}}^n_{j,k}) - \boldsymbol{g}(\bar{\boldsymbol{q}}^n_{j,k-1})}{\Delta y}\right)$$

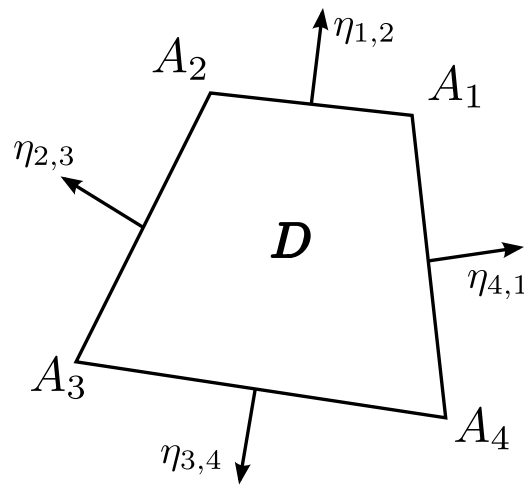

$$\bar{\boldsymbol{q}}_D^{\mathsf{int}} = \frac{1}{|D|} \iint\limits_D \tilde{\boldsymbol{q}}(x, y, t^n)\, dx\, dy - \frac{1}{|D|} \int\limits_{t^n}^{t^{n+1}} \oint\limits_{\partial D} \left[\eta^x \boldsymbol{f}(\boldsymbol{q}) + \eta^y \boldsymbol{g}(\boldsymbol{q})\right] ds\, dt$$

$$\bar{\boldsymbol{q}}_D^{\mathsf{int}} = \bar{\boldsymbol{q}}_D^n - \frac{1}{|D|} \left[\boldsymbol{H}_{12} + \boldsymbol{H}_{23} + \boldsymbol{H}_{34} + \boldsymbol{H}_{41}\right]$$

Projection

We project the intermediate solution, realized in terms of:

the cell averages $\{\bar{\boldsymbol{q}}_D^{\text{int}}\}$ and

the point values at A_1, A_2, A_3 and A_4:

$$\boldsymbol{q}^{n+1}_{j\pm\frac{1}{4},k\pm\frac{1}{4}} = \tilde{\boldsymbol{q}}(\boldsymbol{z}_{j\pm\frac{1}{4},k\pm\frac{1}{4}}, t^n) - \Delta t \left[(\boldsymbol{f}(\boldsymbol{q})_x)^n_{j,k} + (\boldsymbol{g}(\boldsymbol{q})_y)^n_{j,k}\right]$$

onto the original uniform mesh.

To this end, we first use the evolved data to construct a conservative piecewise linear interpolant $\tilde{\boldsymbol{q}}^{\text{int}}(x,y)$, and then integrate it over the original cells $C_{j,k}$ to obtain the cell averages of $\bar{\boldsymbol{q}}$ at the new time level $t = t^{n+1}$:

$$\bar{\boldsymbol{q}}^{n+1}_{j,k} = \frac{1}{\Delta x \Delta y} \iint\limits_{C_{j,k}} \tilde{\boldsymbol{q}}^{\text{int}}(x,y)\, dx\, dy$$

Since $D_{j,k} \subset C_{j,k}$, we take the constant pieces in the central subdomains:

$$\tilde{\boldsymbol{q}}^{\text{int}}(x,y) = \bar{\boldsymbol{q}}^{\text{int}}_{D_{j,k}} \quad \text{for} \quad (x,y) \in D_{j,k}$$

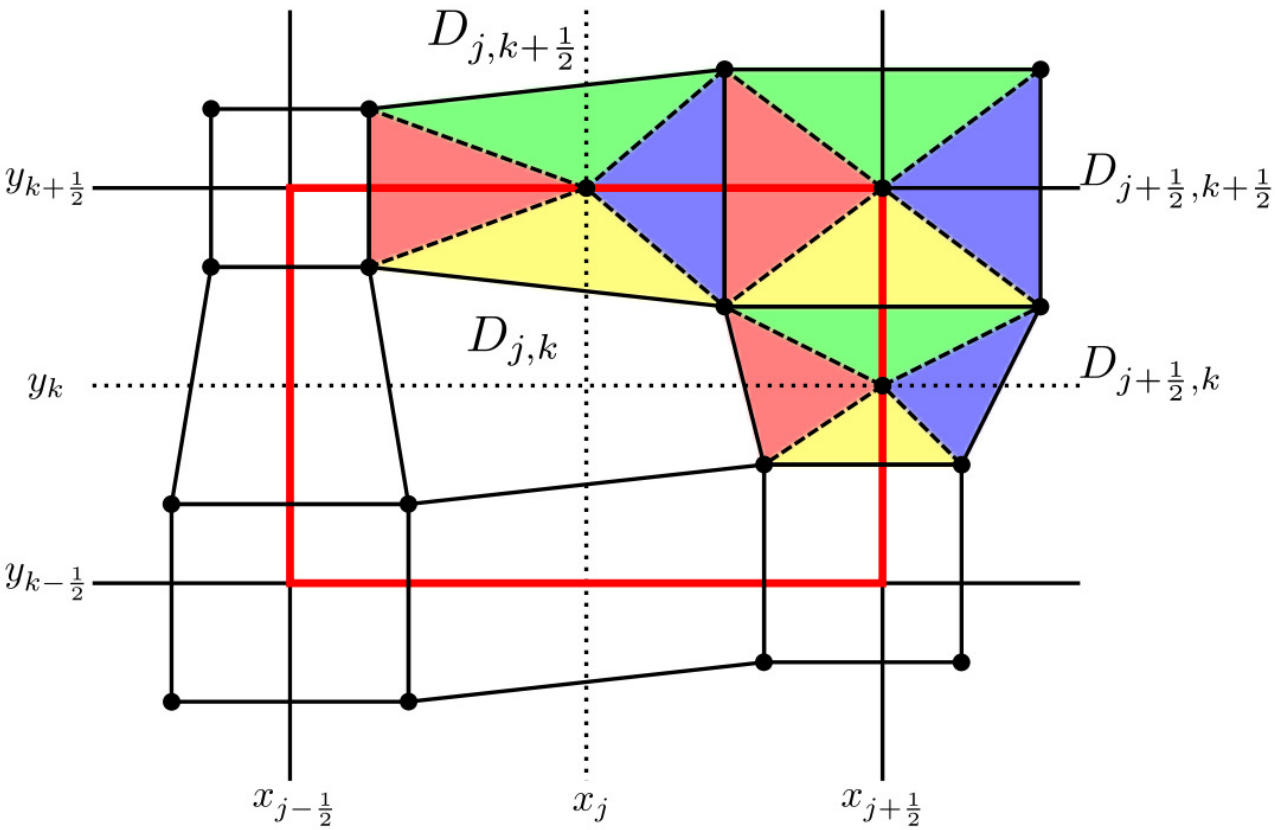

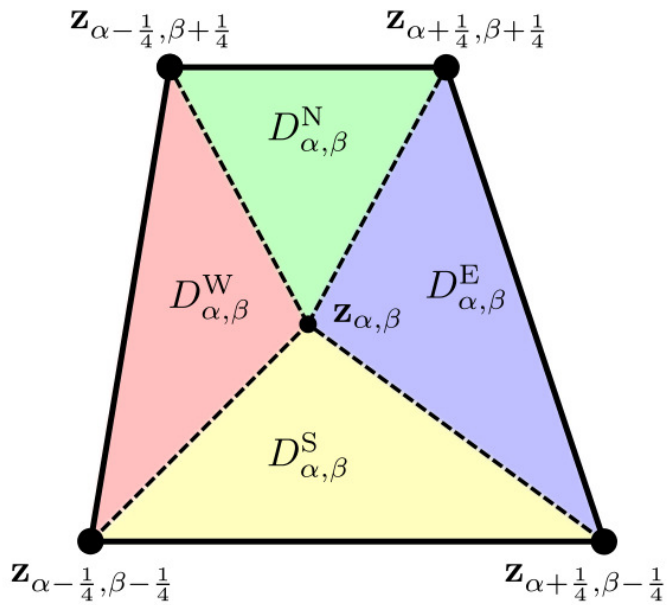

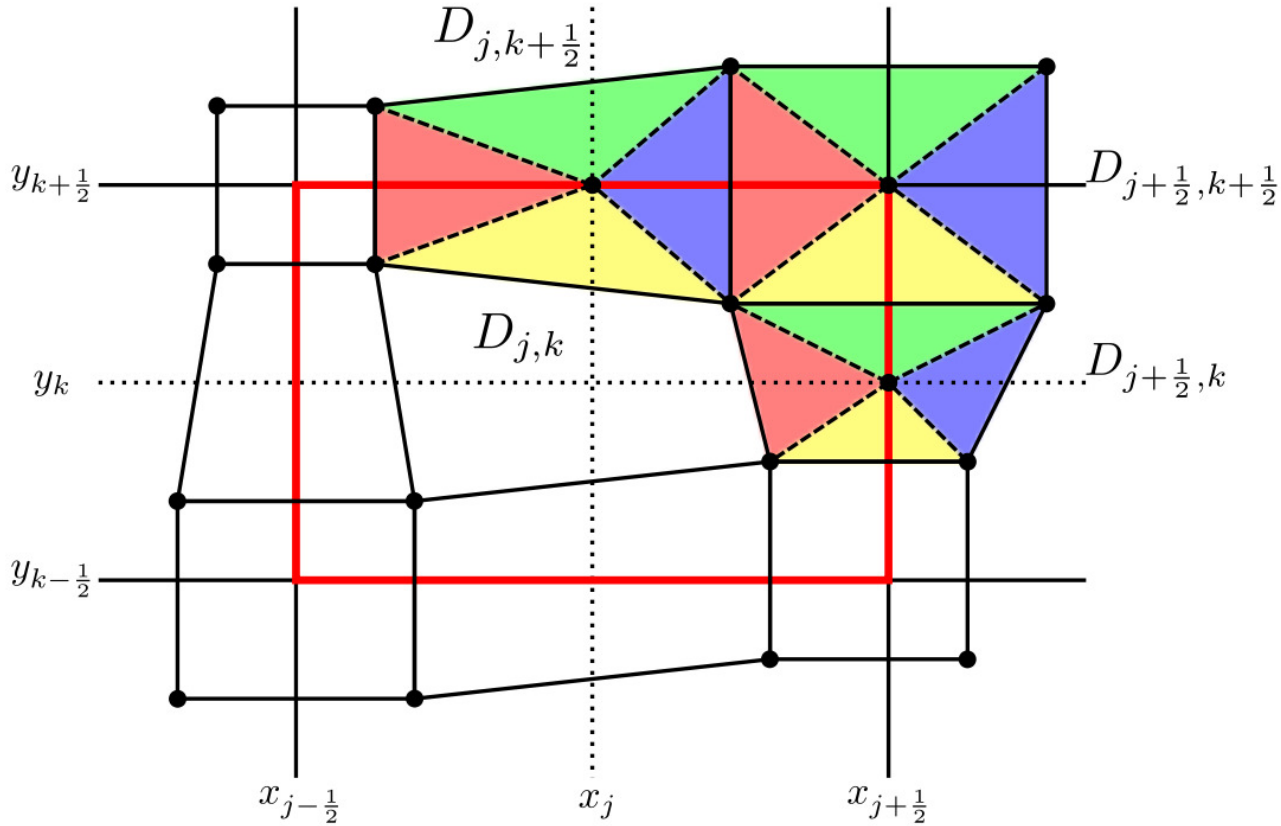

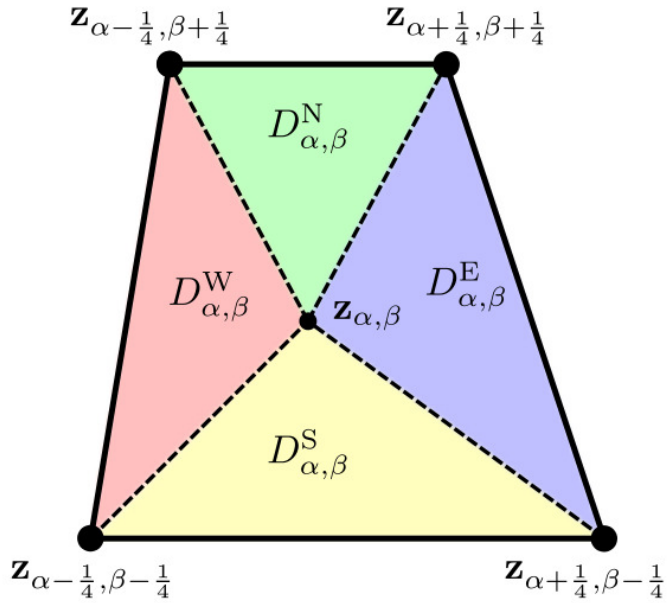

In the domains $D_{\alpha,\beta}$ with $(\alpha,\beta) = (j+\frac{1}{2}, k+\frac{1}{2})$, $(j, k+\frac{1}{2})$ or $(j+\frac{1}{2}, k)$, the interpolant $\widetilde{\boldsymbol{q}}^{\,\mathrm{int}}(x,y)$ consists of four linear pieces that continuously match along the segments connecting (x_α, y_β) with the vertices of $D_{\alpha,\beta}$.

The value of $\widetilde{\boldsymbol{q}}^{\mathsf{int}}$ at (x_α, y_β), which we define by $\boldsymbol{q}_{\alpha,\beta}^{n+1}$, is determined from the conservation requirement:

$$\frac{1}{|D_{\alpha,\beta}|}\iint\limits_{D_{\alpha,\beta}} \widetilde{\boldsymbol{q}}^{\mathsf{int}}(x,y)\,dx\,dy = \bar{\boldsymbol{q}}_{D_{\alpha,\beta}}^{\mathsf{int}}$$

which guarantees the second order of accuracy and results in

$$\begin{aligned}\boldsymbol{q}_{\alpha,\beta}^{n+1} = 3\bar{\boldsymbol{q}}_{D_{\alpha,\beta}}^{\mathsf{int}} &- \frac{|D_{\alpha,\beta}^{\mathsf{N}}| + |D_{\alpha,\beta}^{\mathsf{E}}|}{|D_{\alpha,\beta}|}\boldsymbol{q}_{\alpha+\frac{1}{4},\beta+\frac{1}{4}}^{n+1} - \frac{|D_{\alpha,\beta}^{\mathsf{E}}| + |D_{\alpha,\beta}^{\mathsf{S}}|}{|D_{\alpha,\beta}|}\boldsymbol{q}_{\alpha+\frac{1}{4},\beta-\frac{1}{4}}^{n+1}\\ &- \frac{|D_{\alpha,\beta}^{\mathsf{S}}| + |D_{\alpha,\beta}^{\mathsf{W}}|}{|D_{\alpha,\beta}|}\boldsymbol{q}_{\alpha-\frac{1}{4},\beta-\frac{1}{4}}^{n+1} - \frac{|D_{\alpha,\beta}^{\mathsf{W}}| + |D_{\alpha,\beta}^{\mathsf{N}}|}{|D_{\alpha,\beta}|}\boldsymbol{q}_{\alpha-\frac{1}{4},\beta+\frac{1}{4}}^{n+1}\end{aligned}$$

The constructed interpolant $\tilde{\boldsymbol{q}}^{\text{int}}(x,y)$ may be oscillatory. In order to avoid appearance on new local extrema at (x_α, y_β), we check whether

$$(q^{(i)})^{n+1}_{\alpha,\beta} > \max\left\{(\bar{q}^{(i)})^{\text{int}}_{D_{\alpha,\beta}},\ (\bar{q}^{(i)})^{\text{int}}_{D_{\alpha\pm\frac{1}{2},\beta}},\ (\bar{q}^{(i)})^{\text{int}}_{D_{\alpha,\beta\pm\frac{1}{2}}}\right\}$$

or

$$(q^{(i)})^{n+1}_{\alpha,\beta} < \min\left\{(\bar{q}^{(i)})^{\text{int}}_{D_{\alpha,\beta}},\ (\bar{q}^{(i)})^{\text{int}}_{D_{\alpha\pm\frac{1}{2},\beta}},\ (\bar{q}^{(i)})^{\text{int}}_{D_{\alpha,\beta\pm\frac{1}{2}}}\right\}$$

for some component i of $\boldsymbol{q}$, and then replace the corresponding piecewise linear approximations with

$$(\tilde{q}^{(i)})^{\text{int}}(x,y) = (\bar{q}^{(i)})^{\text{int}}_{D_{\alpha,\beta}} \quad \text{for} \quad (x,y) \in D_{\alpha,\beta}$$

Remark. This reconstruction correction procedure locally reduces the order of the interpolant $\tilde{\boldsymbol{q}}^{\text{int}}$ to the first one, but this is the same clipping effect as in the case of the minmod limiter.

2-D Semi-Discrete Central-Upwind Scheme

Similar to the 1-D case, a 2-D semi-discrete central-upwind scheme can be rigorously derived from the fully discrete scheme.

Rectangular Grid

[Kurganov, Petrova; 2001] [Kurganov, Noelle, Petrova; 2001]

[Kurganov, Tadmor; 2002] [Kurganov, Lin; 2007]

Triangular Grid

[Kurganov, Petrova; 2005]

Quadrilateral and Polygonal Grids

Beljadid, Kurganov, Mohammadian, Seidou, Shirkhani

Scheme from [Kurganov, Tadmor; 2002]

$$\frac{d}{dt}\bar{\boldsymbol{q}}_{j,k}(t) = -\frac{\boldsymbol{H}^x_{j+\frac{1}{2},k}(t) - \boldsymbol{H}^x_{j-\frac{1}{2},k}(t)}{\Delta x} - \frac{\boldsymbol{H}^y_{j,k+\frac{1}{2}}(t) - \boldsymbol{H}^y_{j,k-\frac{1}{2}}(t)}{\Delta y}$$

$$\boldsymbol{H}^x_{j+\frac{1}{2},k}(t) = \frac{a^+_{j+\frac{1}{2},k}\boldsymbol{f}(\boldsymbol{q}^{\mathsf{E}}_{j,k}) - a^-_{j+\frac{1}{2},k}\boldsymbol{f}(\boldsymbol{q}^{\mathsf{W}}_{j+1,k})}{a^+_{j+\frac{1}{2},k} - a^-_{j+\frac{1}{2},k}} + \frac{a^+_{j+\frac{1}{2},k}a^-_{j+\frac{1}{2},k}}{a^+_{j+\frac{1}{2},k} - a^-_{j+\frac{1}{2},k}}\left(\boldsymbol{q}^{\mathsf{W}}_{j+1,k} - \boldsymbol{q}^{\mathsf{E}}_{j,k}\right)$$

$$\boldsymbol{H}^y_{j,k+\frac{1}{2}}(t) = \frac{b^+_{j,k+\frac{1}{2}}\boldsymbol{g}(\boldsymbol{q}^{\mathsf{N}}_{j,k}) - b^-_{j,k+\frac{1}{2}}\boldsymbol{g}(\boldsymbol{q}^{\mathsf{S}}_{j,k+1})}{b^+_{j,k+\frac{1}{2}} - b^-_{j,k+\frac{1}{2}}} + \frac{b^+_{j,k+\frac{1}{2}}b^-_{j,k+\frac{1}{2}}}{b^+_{j,k+\frac{1}{2}} - b^-_{j,k+\frac{1}{2}}}\left(\boldsymbol{q}^{\mathsf{S}}_{j,k+1} - \boldsymbol{q}^{\mathsf{N}}_{j,k}\right)$$

Gas Dynamics

$$\frac{\partial}{\partial t}\begin{bmatrix}\rho\\ \rho u\\ \rho v\\ E\end{bmatrix}+\frac{\partial}{\partial x}\begin{bmatrix}\rho u\\ \rho u^2+p\\ \rho uv\\ u(E+p)\end{bmatrix}+\frac{\partial}{\partial y}\begin{bmatrix}\rho v\\ \rho uv\\ \rho v^2+p\\ v(E+p)\end{bmatrix}=0$$

$p=(\gamma-1)\left[E-\frac{\rho}{2}(u^2+v^2)\right]$: equation of state

ρ: density

u, v: x- and y-velocities

p: pressure

E: total energy, respectively

$\gamma=1.4$

Example — Explosion

$$(\rho, u, v, p)\Big|_{(x,y,0)} = \begin{cases} (1.000, 0, 0, 1.0), & x^2 + y^2 < 0.16 \\ (0.125, 0, 0, 0.1), & \text{otherwise} \end{cases}$$

By $t = 3.2$ the circular contact curve typically develops instabilities. Therefore, this example is a good test for the amount of numerical dissipation present in the studied schemes.

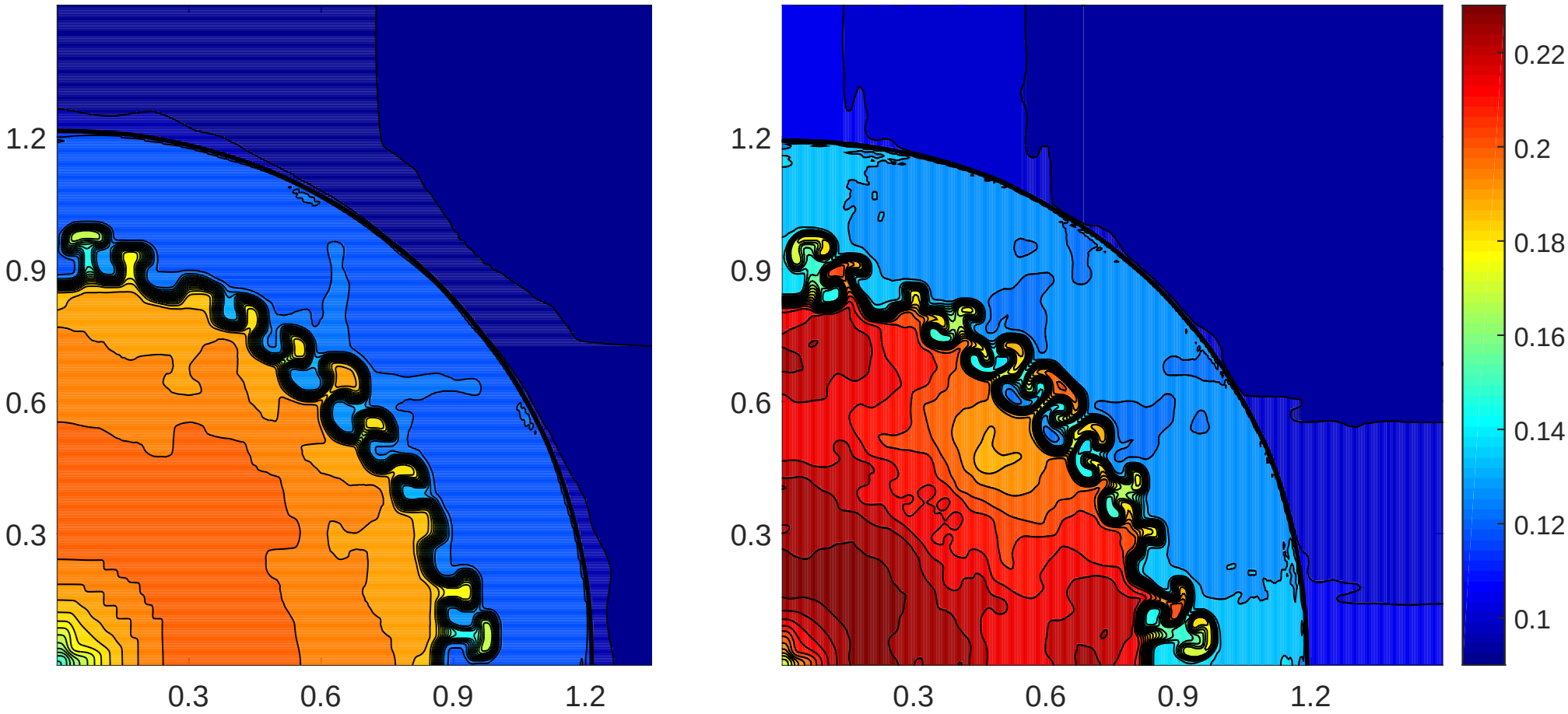

Semi-discrete (left) vs. fully discrete (right)

Example — Implosion

$$(\rho(x,y,0), u(x,y,0), v(x,y,0), p(x,y,0)) = \begin{cases} (0.125, 0, 0, 0.14), & |x| + |y| < 0.15 \\ (1.000, 0, 0, 1.00), & \text{otherwise.} \end{cases}$$

We set the solid wall boundary conditions.

A jet of liquid is expected to emerge. However, the numerical dissipation present in many second-order schemes may smear the jet.

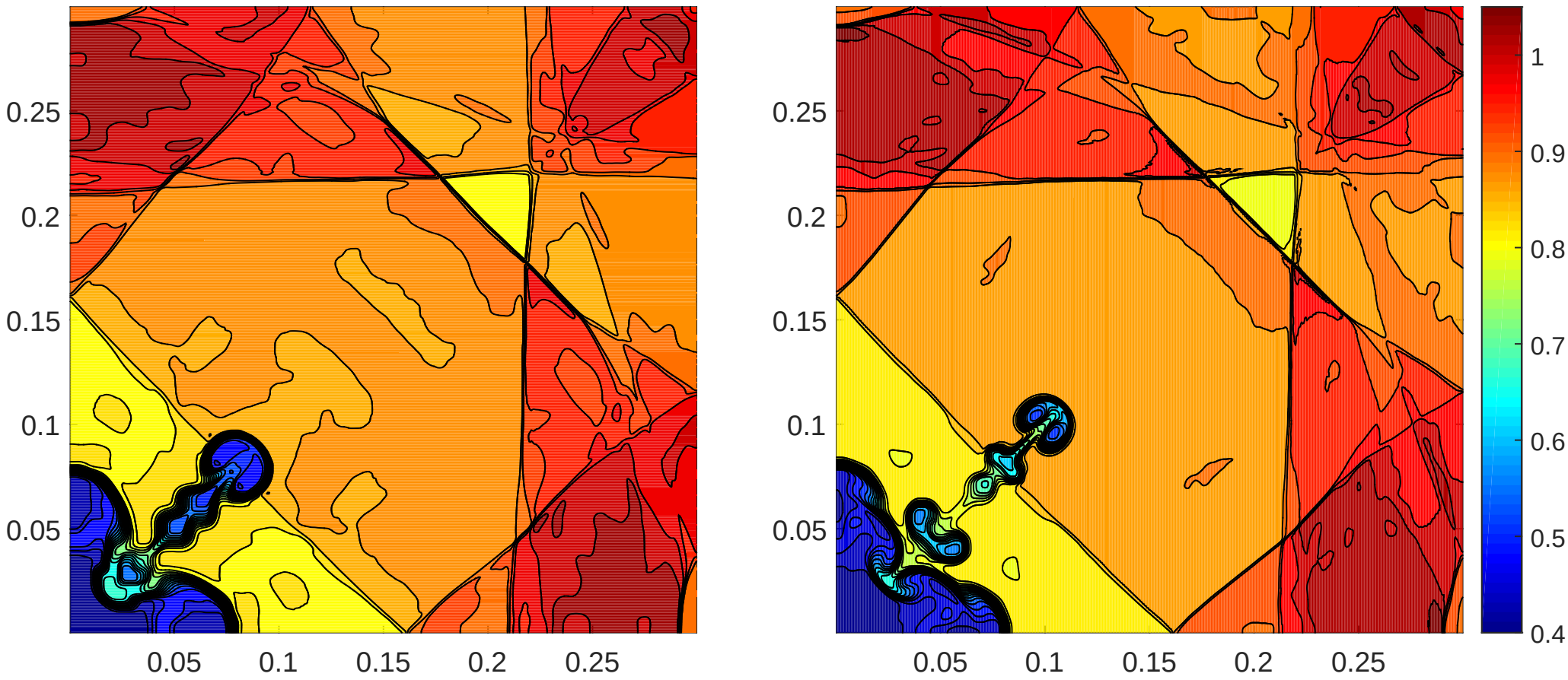

Semi-discrete (left) vs. fully discrete (right)

Back to 1-D Gas Dynamics

[Kurganov; in preparation]

$$\frac{\partial}{\partial t}\begin{bmatrix}\rho\\ \rho u\\ E\end{bmatrix}+\frac{\partial}{\partial x}\begin{bmatrix}\rho u\\ \rho u^2+p\\ u(E+p)\end{bmatrix}=0$$

$p=(\gamma-1)\left[E-\frac{\rho u^2}{2}\right]$: equation of state

ρ: density

u: velocity

p: pressure

E: total energy

$\gamma=1.4$

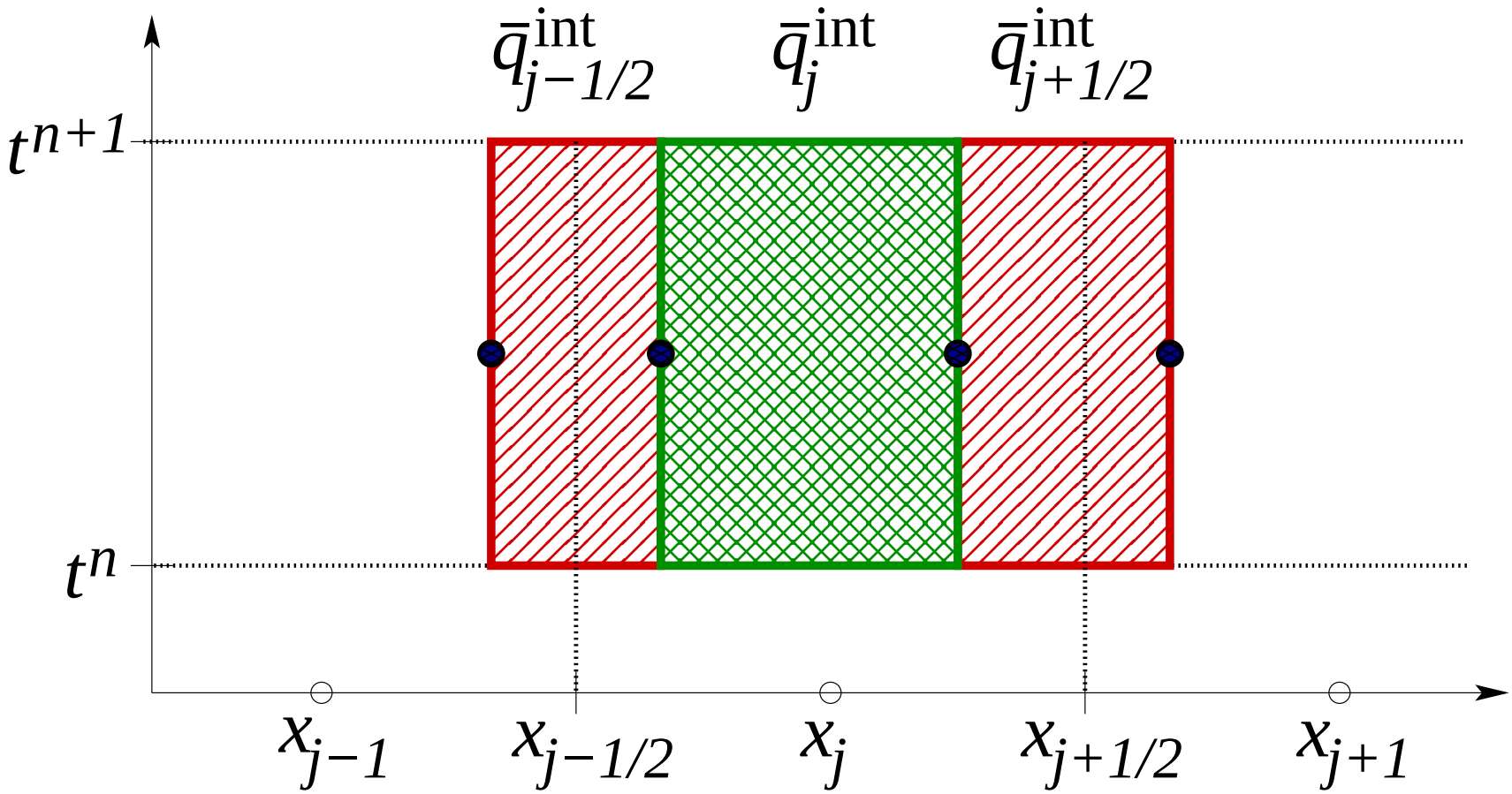
$\bar{q}^{\text{int}}_{j-1/2}$
$\bar{q}^{\text{int}}_{j}$
$\bar{q}^{\text{int}}_{j+1/2}$
t^{n+1}
t^{n}
x_{j-1}
$x_{j-1/2}$
x_{j}
$x_{j+1/2}$
x_{j+1}

Idea: **Modify the projection step**

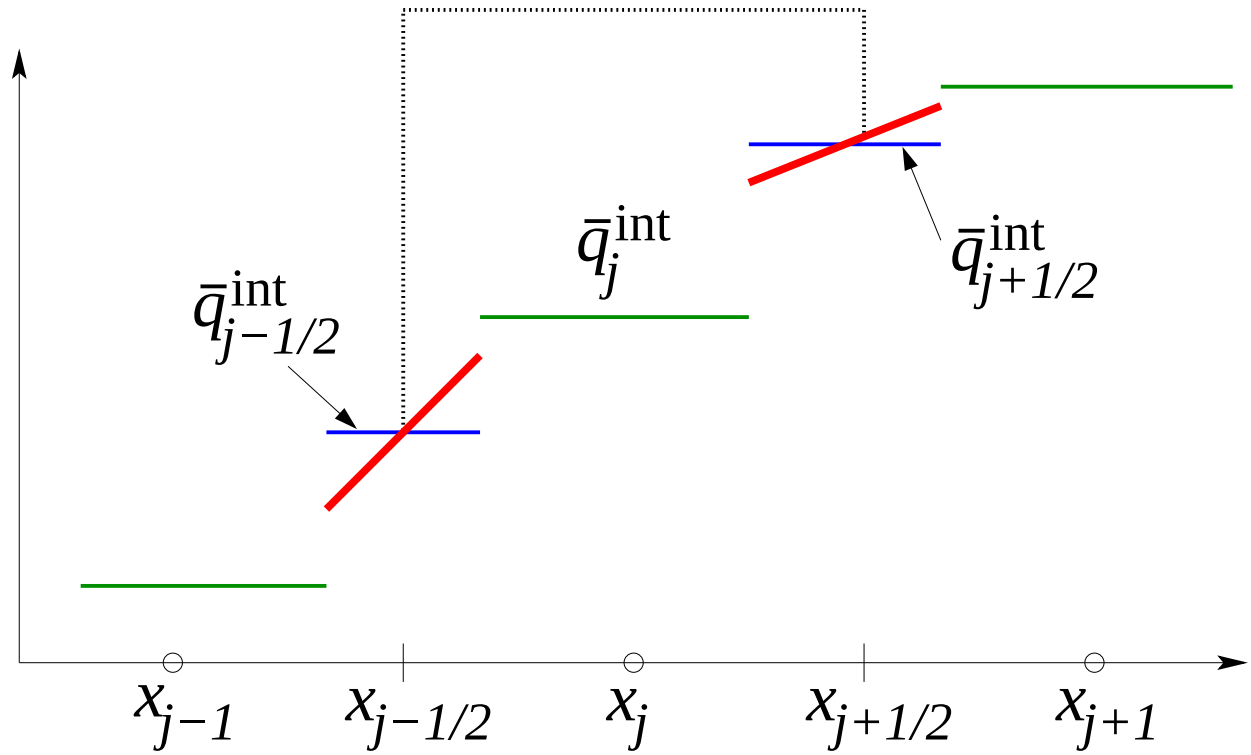

- The solution is averaged over the Riemann fans

- All conservative variables remain continuous in the cell $(x^{\ell}_{j+\frac{1}{2}}, x^{r}_{j+\frac{1}{2}})$

This brings excessive numerical dissipation!

In principle, a better approximation of $\boldsymbol{q}^{\text{int}}$ in the cell $(x^{\ell}_{j+\frac{1}{2}}, x^{r}_{j+\frac{1}{2}})$ can be obtained by incorporating the wave propagation information into the interpolant. However, this approach will require the solution of the (generalized) Riemann problem.

Alternatively, recall that our goal is to derive a semi-discrete scheme, that is, to pass to the $\Delta t \to 0$ limit, in which case the interval $(x^{\ell}_{j+\frac{1}{2}}, x^{r}_{j+\frac{1}{2}})$ shrinks into a point where $\boldsymbol{q}^{\text{int}}$ may have at most two one-sided values.

We therefore replace the intermediate piece $\bar{\boldsymbol{q}}^{\text{int}}_{j+\frac{1}{2}}$ with two constant pieces, $\bar{\boldsymbol{q}}^{\text{int,L}}_{j+\frac{1}{2}}$ and $\bar{\boldsymbol{q}}^{\text{int,R}}_{j+\frac{1}{2}}$.

That is, instead of

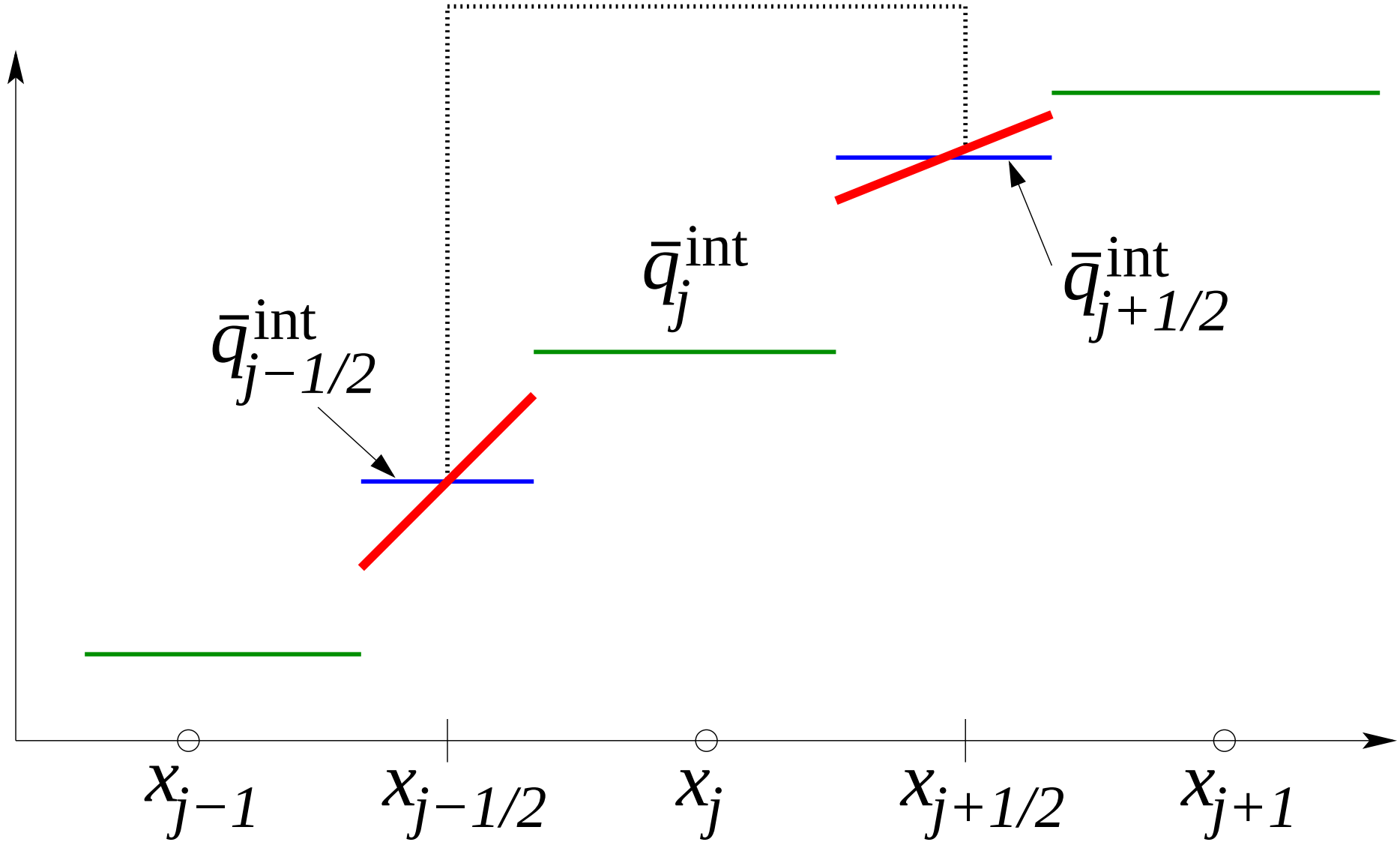

we perform the projection as follows:

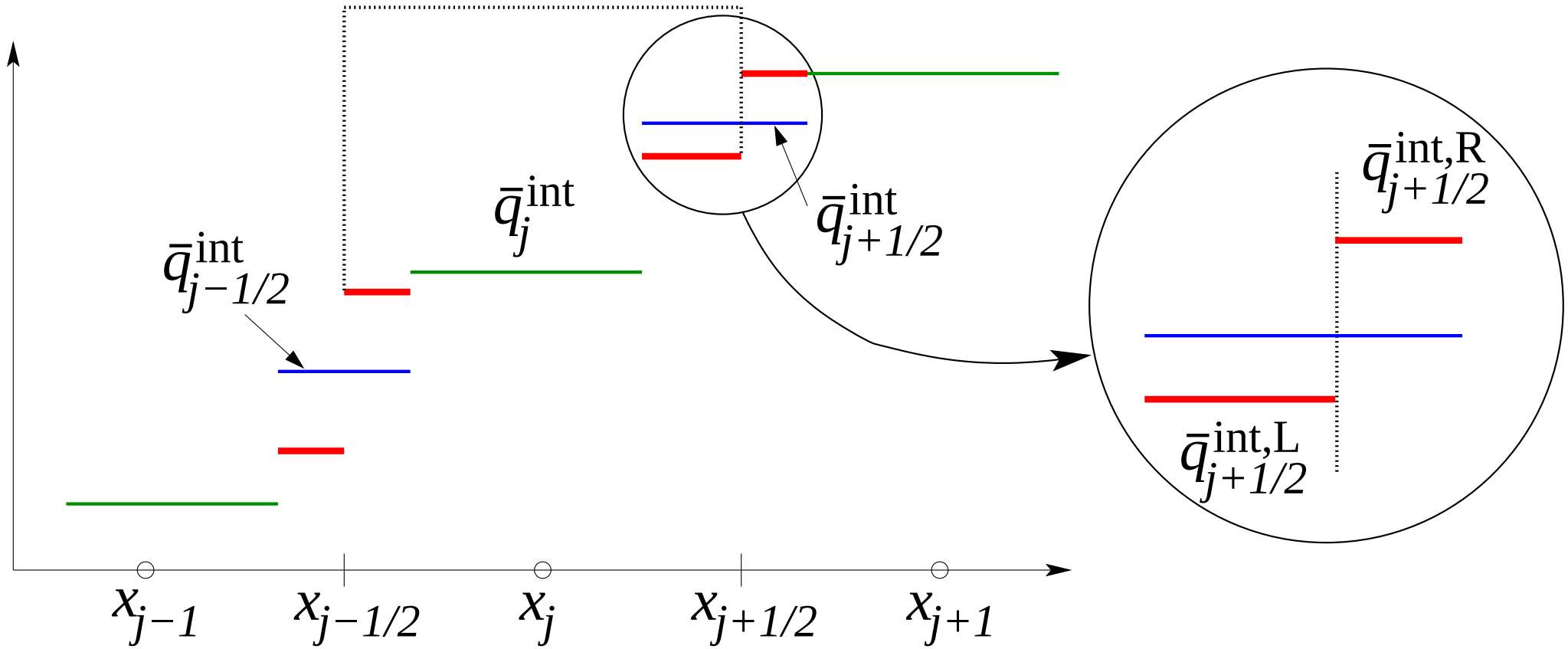

For the compressible Euler equations:

$$\bar{\boldsymbol{q}}^{\text{int,L}}_{j+\frac{1}{2}} = \left(\bar{\rho}^{\text{int,L}}_{j+\frac{1}{2}}, \overline{m}^{\text{int,L}}_{j+\frac{1}{2}}, \overline{E}^{\text{int,L}}_{j+\frac{1}{2}}\right)^T \quad \text{and} \quad \bar{\boldsymbol{q}}^{\text{int,R}}_{j+\frac{1}{2}} = \left(\bar{\rho}^{\text{int,R}}_{j+\frac{1}{2}}, \overline{m}^{\text{int,R}}_{j+\frac{1}{2}}, \overline{E}^{\text{int,R}}_{j+\frac{1}{2}}\right)^T$$

represent six pieces of information, which can be used to adjust the projection step.

For instance, one can enforce continuity of the velocity and pressure (which are continuous across contact discontinuities!) by setting

$$u^{\text{int,L}}_{j+\frac{1}{2}} = u^{\text{int,R}}_{j+\frac{1}{2}}, \qquad p^{\text{int,L}}_{j+\frac{1}{2}} = p^{\text{int,R}}_{j+\frac{1}{2}}$$

This together with three conservation requirements,

$$\bar{\boldsymbol{q}}^{\text{int,R}}_{j+\frac{1}{2}} a^{+}_{j+\frac{1}{2}} - \bar{\boldsymbol{q}}^{\text{int,L}}_{j+\frac{1}{2}} a^{-}_{j+\frac{1}{2}} = \bar{\boldsymbol{q}}^{\text{int}}_{j+\frac{1}{2}} (a^{+}_{j+\frac{1}{2}} - a^{-}_{j+\frac{1}{2}})$$

result in five equations to be satisfied.

The remaining degree of freedom can be used for obtaining a sharper approximation of $\boldsymbol{q}^{\text{int}}$.

For example, one can make the value of $\bar{\rho}^{\text{int,R}}_{j+\frac{1}{2}} - \bar{\rho}^{\text{int,L}}_{j+\frac{1}{2}}$ as close as possible to $\bar{\rho}^{\text{int}}_{j+1} - \bar{\rho}^{\text{int}}_{j}$ without sacrificing the monotonicity of ρ:

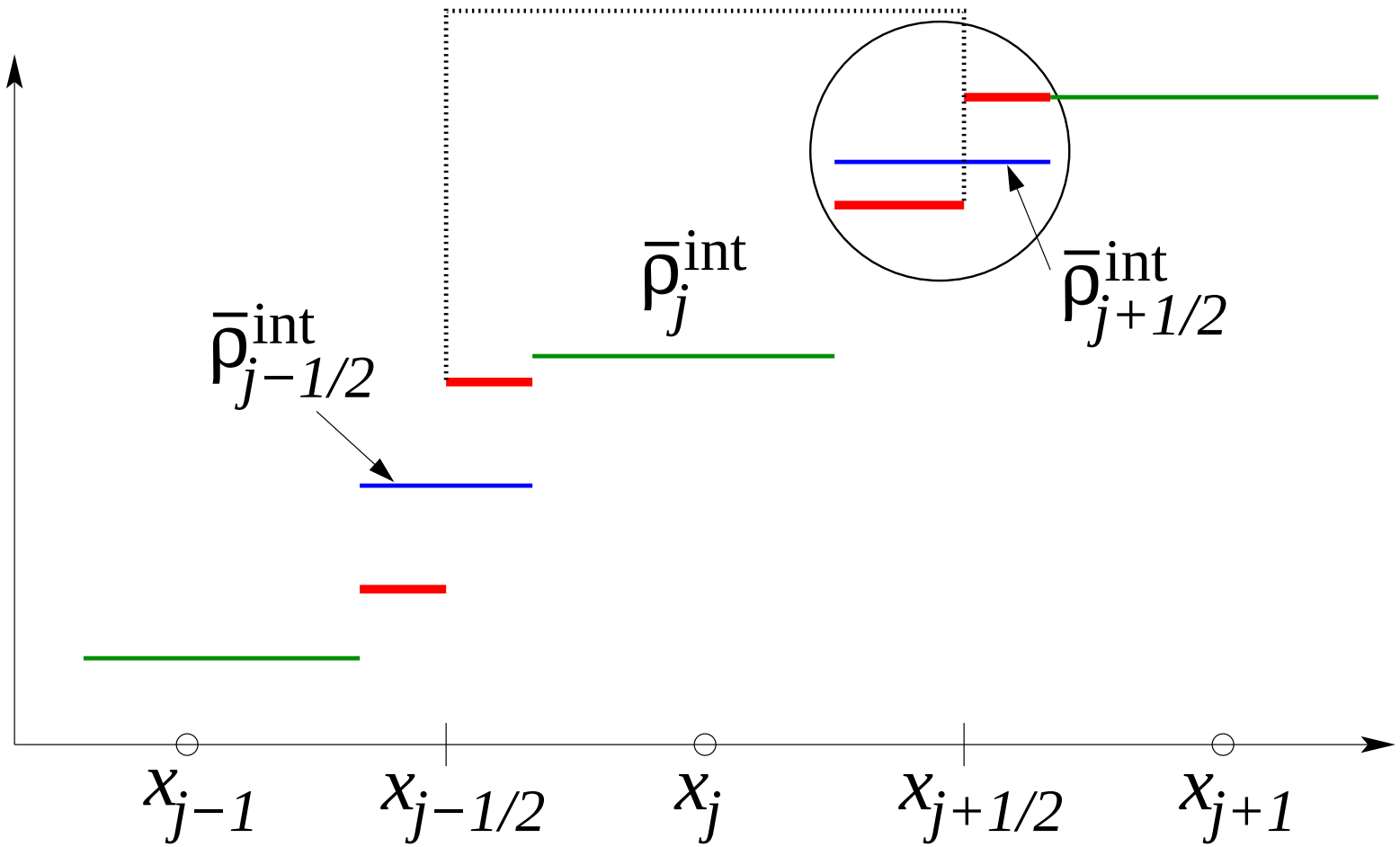

The new projection procedure leads to the same semi-discrete central-upwind scheme

$$\frac{d}{dt}\bar{\boldsymbol{q}}_j(t) = -\frac{\boldsymbol{H}_{j+\frac{1}{2}}(t) - \boldsymbol{H}_{j-\frac{1}{2}}(t)}{\Delta x}$$

$$\boldsymbol{H}_{j+\frac{1}{2}} = \frac{a^+_{j+\frac{1}{2}}\boldsymbol{f}(\boldsymbol{q}^-_{j+\frac{1}{2}}) - a^-_{j+\frac{1}{2}}\boldsymbol{f}(\boldsymbol{q}^+_{j+\frac{1}{2}})}{a^+_{j+\frac{1}{2}} - a^-_{j+\frac{1}{2}}} + \frac{a^+_{j+\frac{1}{2}}a^-_{j+\frac{1}{2}}}{a^+_{j+\frac{1}{2}} - a^-_{j+\frac{1}{2}}}\left(\boldsymbol{q}^+_{j+\frac{1}{2}} - \boldsymbol{q}^-_{j+\frac{1}{2}}\right) - \boxed{\boldsymbol{d}_{j+\frac{1}{2}}}$$

but with the modified "anti-diffusion" term:

$$\boldsymbol{d}_{j+\frac{1}{2}} = -\text{minmod}\left(a^{+}_{j+\frac{1}{2}}(\rho^{+}_{j+\frac{1}{2}} - \rho^{*}_{j+\frac{1}{2}}), -a^{-}_{j+\frac{1}{2}}(\rho^{*}_{j+\frac{1}{2}} - \rho^{-}_{j+\frac{1}{2}})\right)\begin{pmatrix} 1 \\ u^{*}_{j+\frac{1}{2}} \\ \frac{(u^{*}_{j+\frac{1}{2}})^2}{2} \end{pmatrix}$$

$$\boldsymbol{q}^{*}_{j+\frac{1}{2}} = \frac{a^{+}_{j+\frac{1}{2}}\boldsymbol{q}^{+}_{j+\frac{1}{2}} - a^{-}_{j+\frac{1}{2}}\boldsymbol{q}^{-}_{j+\frac{1}{2}} - \left\{\boldsymbol{f}(\boldsymbol{q}^{+}_{j+\frac{1}{2}}) - \boldsymbol{f}(\boldsymbol{q}^{-}_{j+\frac{1}{2}})\right\}}{a^{+}_{j+\frac{1}{2}} - a^{-}_{j+\frac{1}{2}}}$$

Example — Moving Contact Wave

Initial data:

$$(\rho, u, p)(x, 0) = \begin{cases} (1.4, 0.1, 1), & x < 0.3 \\ (1.0, 0.1, 1), & x > 0.3 \end{cases}$$

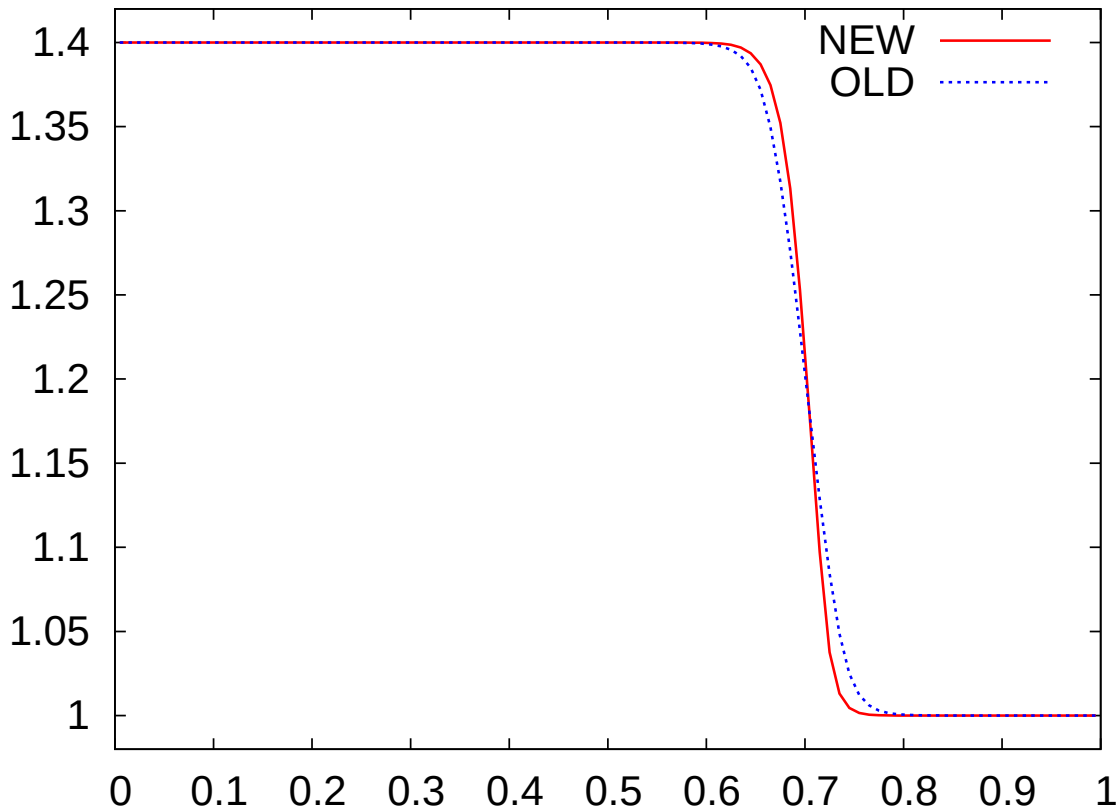

Example — Stationary Contact Wave, Traveling Shock and Rarefaction

$$\frac{\partial}{\partial t}\begin{bmatrix} \rho \\ \rho u \\ E \end{bmatrix} + \frac{\partial}{\partial x}\begin{bmatrix} \rho u \\ \rho u^2 + p \\ u(E+p) \end{bmatrix} = 0$$

$$p = (\gamma - 1)\left[E - \frac{\rho u^2}{2}\right]$$

Initial data:

$$(\rho, u, p)(x, 0) = \begin{cases} (1, -19.59745, 1000), & x < 0.8 \\ (1, -19.59745, 0.01), & x > 0.8 \end{cases}$$

Final time: $t = 0.03$

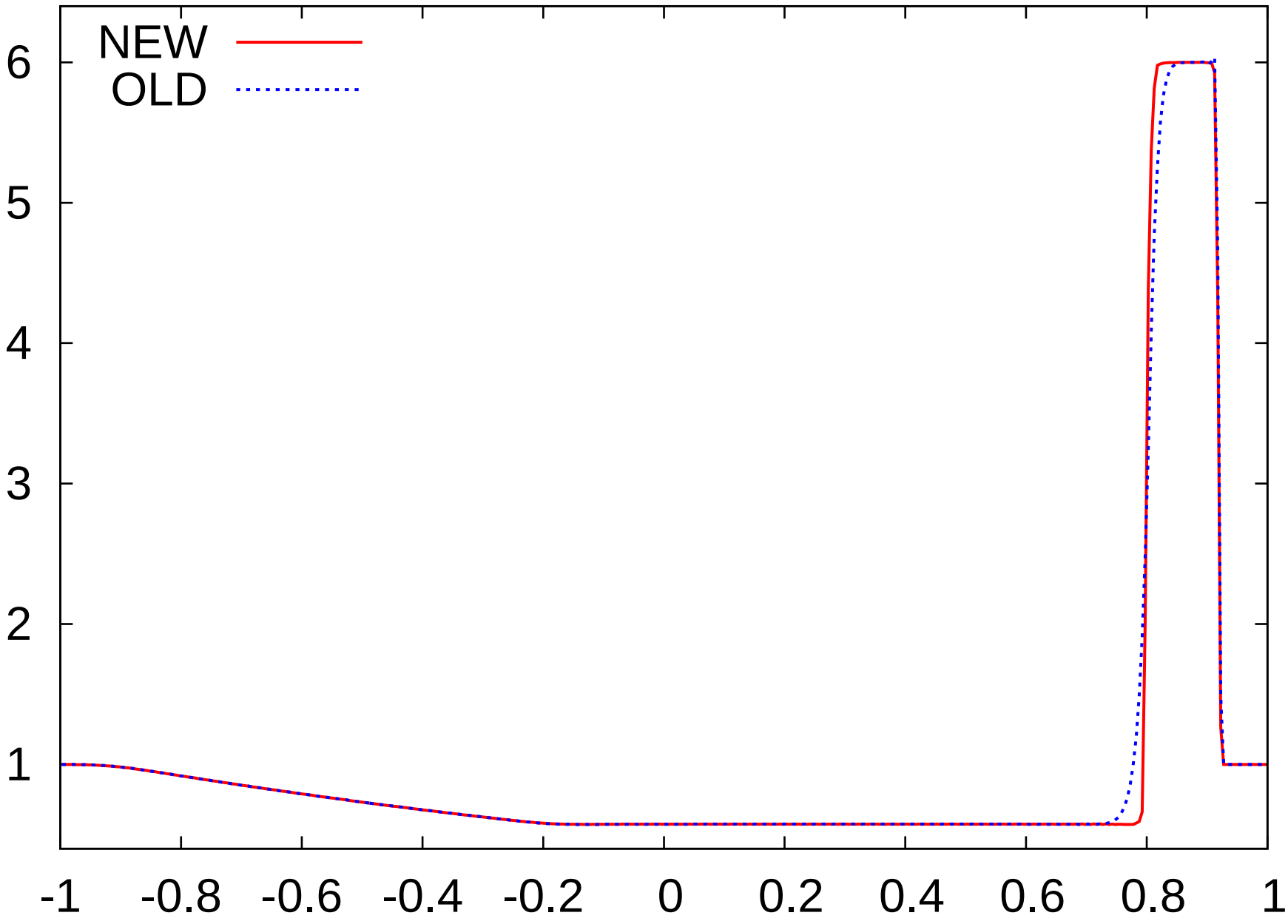
NEW
OLD
6
5
4
3
2
1
-1
-0.8
-0.6
-0.4
-0.2
0
0.2
0.4
0.6
0.8
1

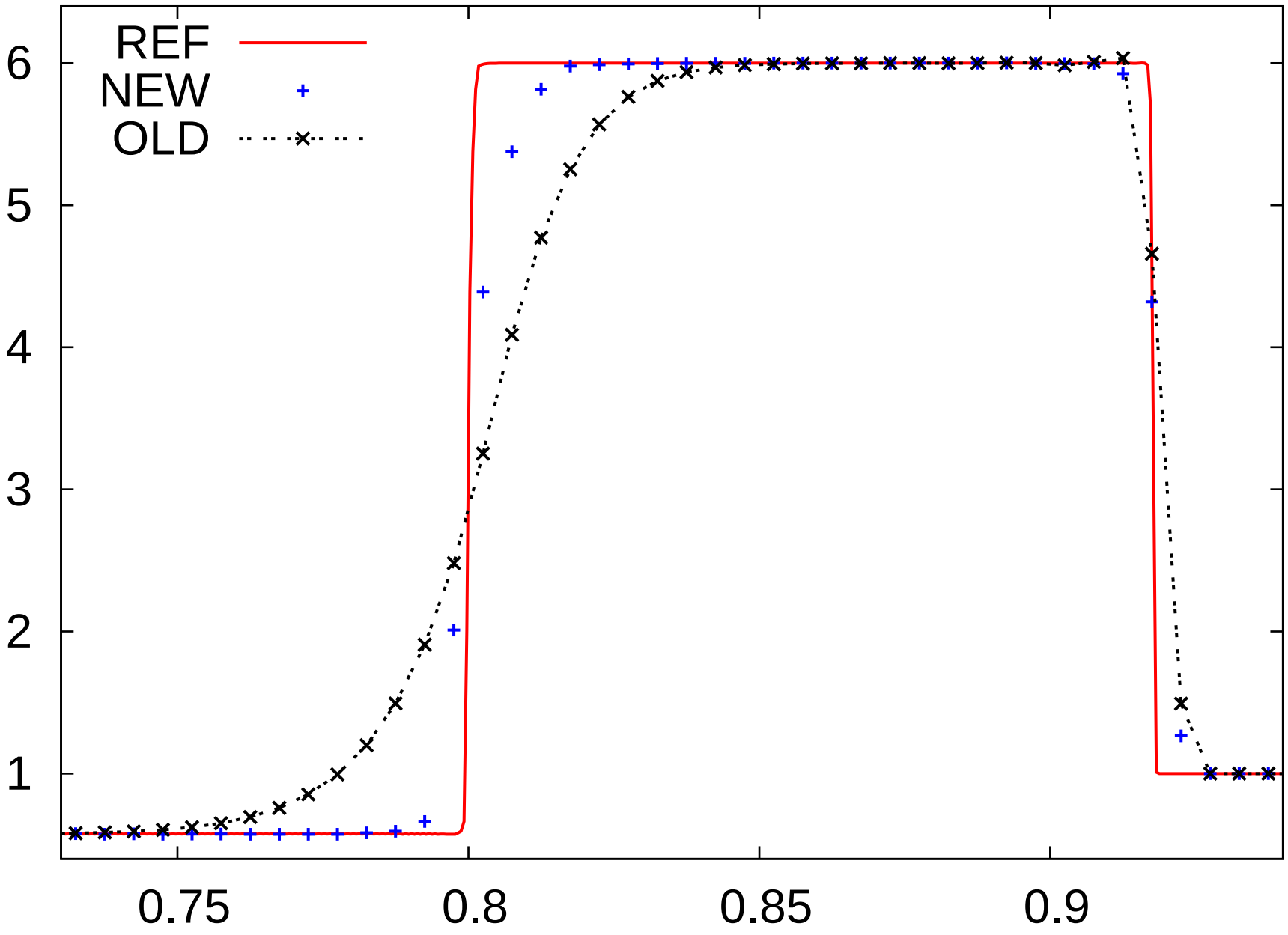
REF
NEW
OLD
6
5
4
3
2
1
0.75
0.8
0.85
0.9

Example — "Shock-Bubble" Interaction

The initial data correspond to a left-moving shock, initially located at $x = 0.75$, and a "bubble" with radius 0.25, initially located at the origin:

$$(\rho, u, p)(x, y, 0) = \begin{cases} (13.1538, 0, 1), & |x| < 0.25 \\ (1.3333, -0.3535, 1.5), & x > 0.75 \\ (1, 0, 1), & \text{otherwise} \end{cases}$$

Solid wall boundary condition on the right.

Final time $t = 3$.

Density, $\Delta x = 1/100$

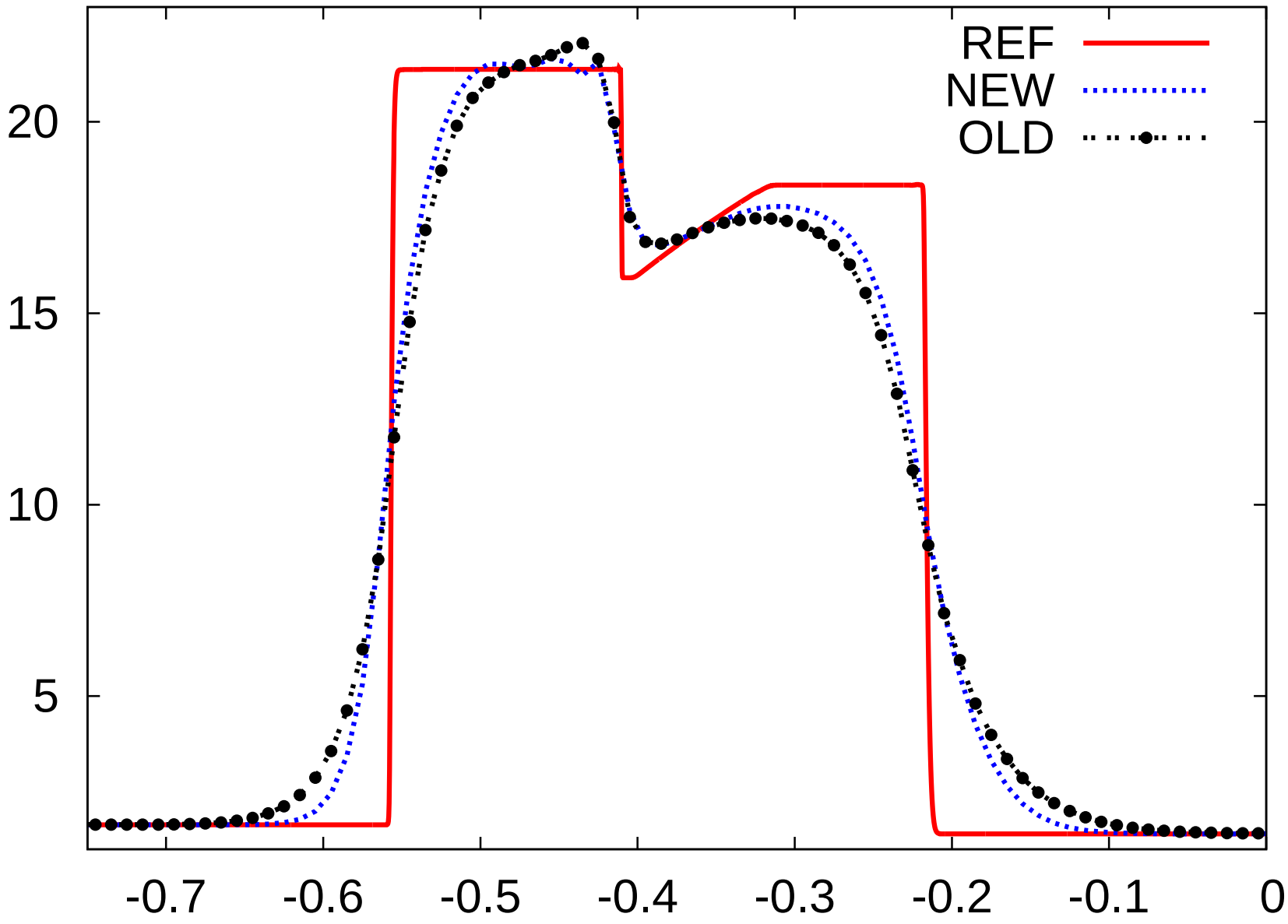

Velocity, $\Delta x = 1/100$

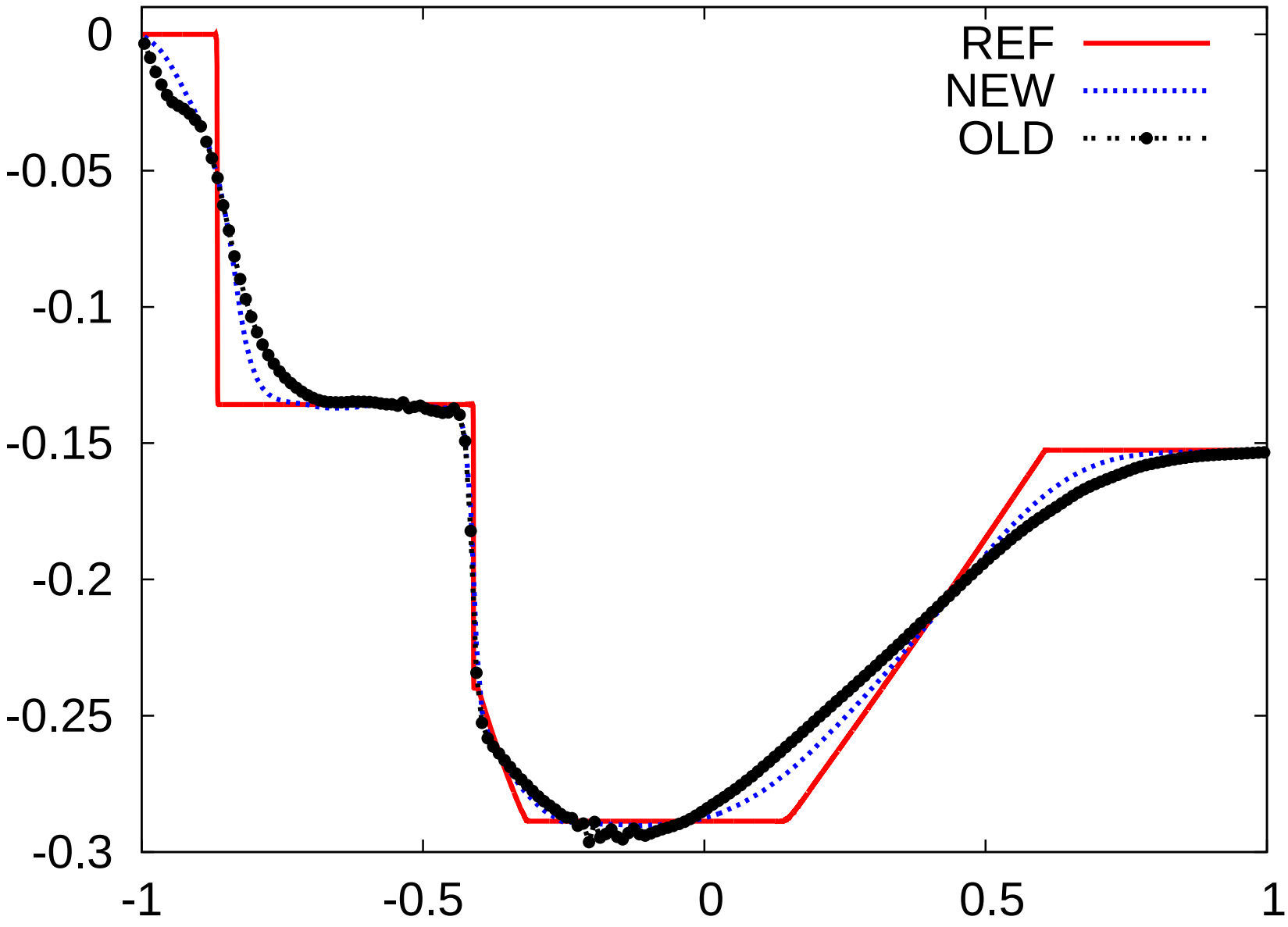

Pressure, $\Delta x = 1/100$

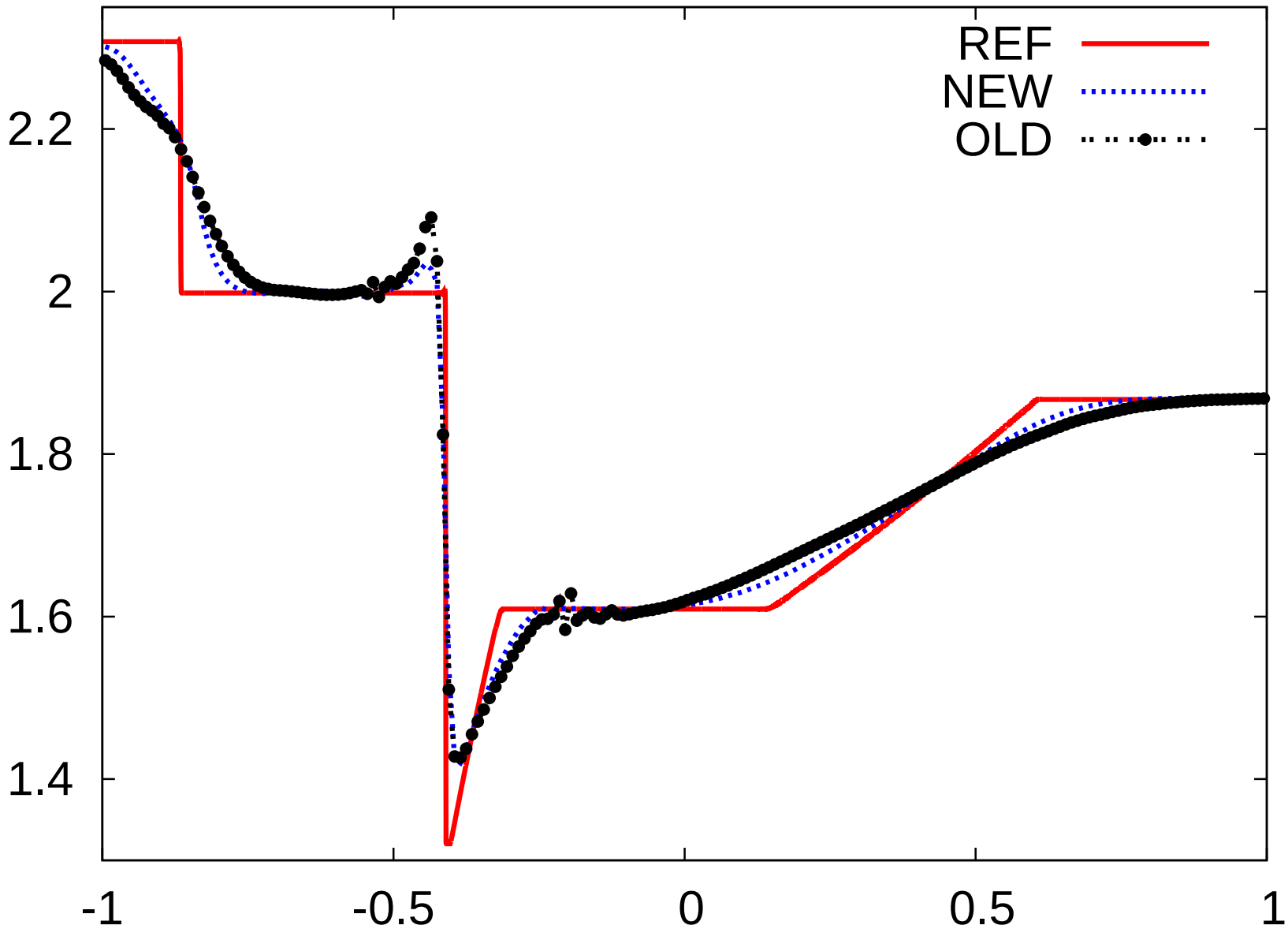

Density, $\Delta x = 1/200$

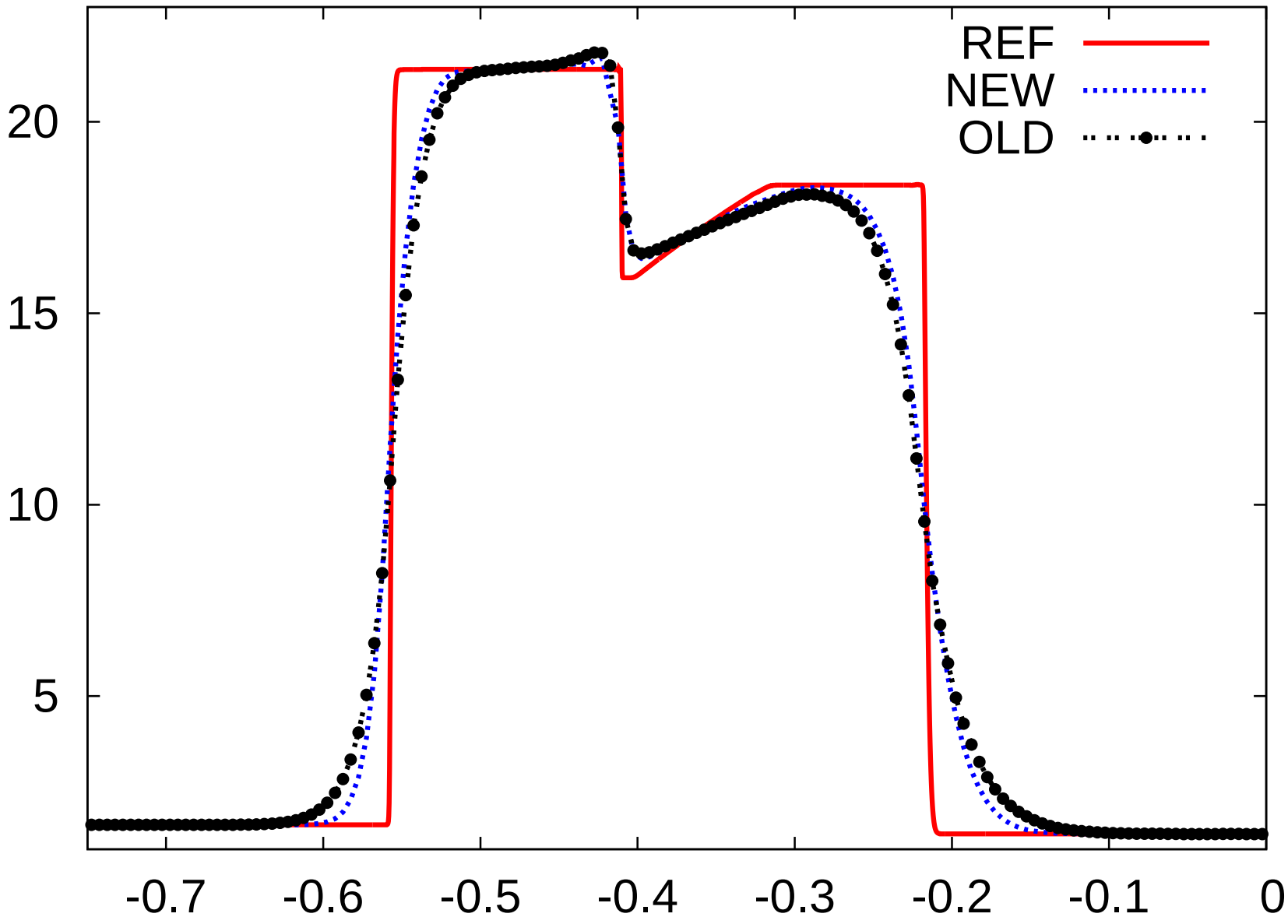

Velocity, $\Delta x = 1/200$

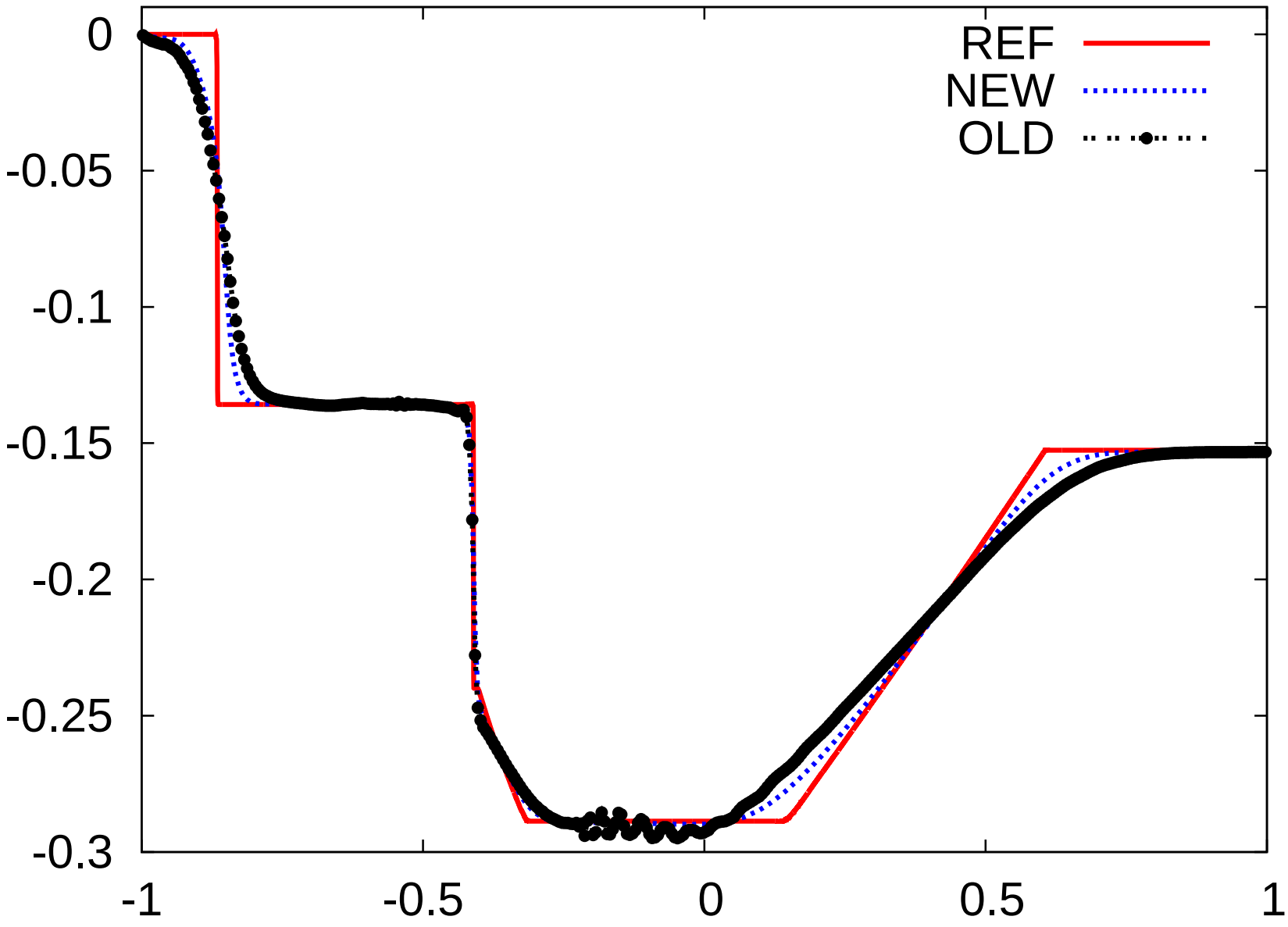

Pressure, $\Delta x = 1/200$

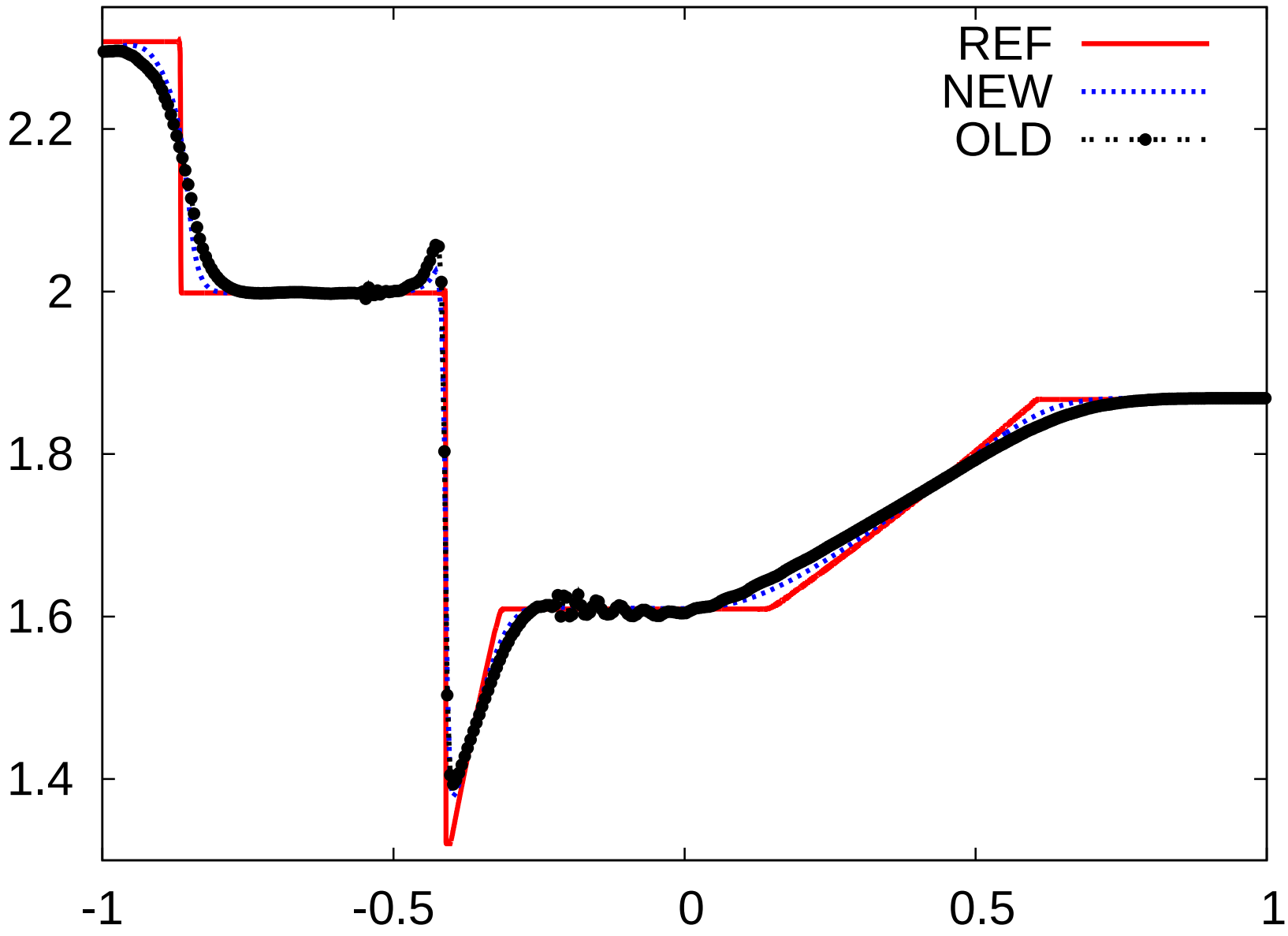

Velocity, $\Delta x = 1/200$

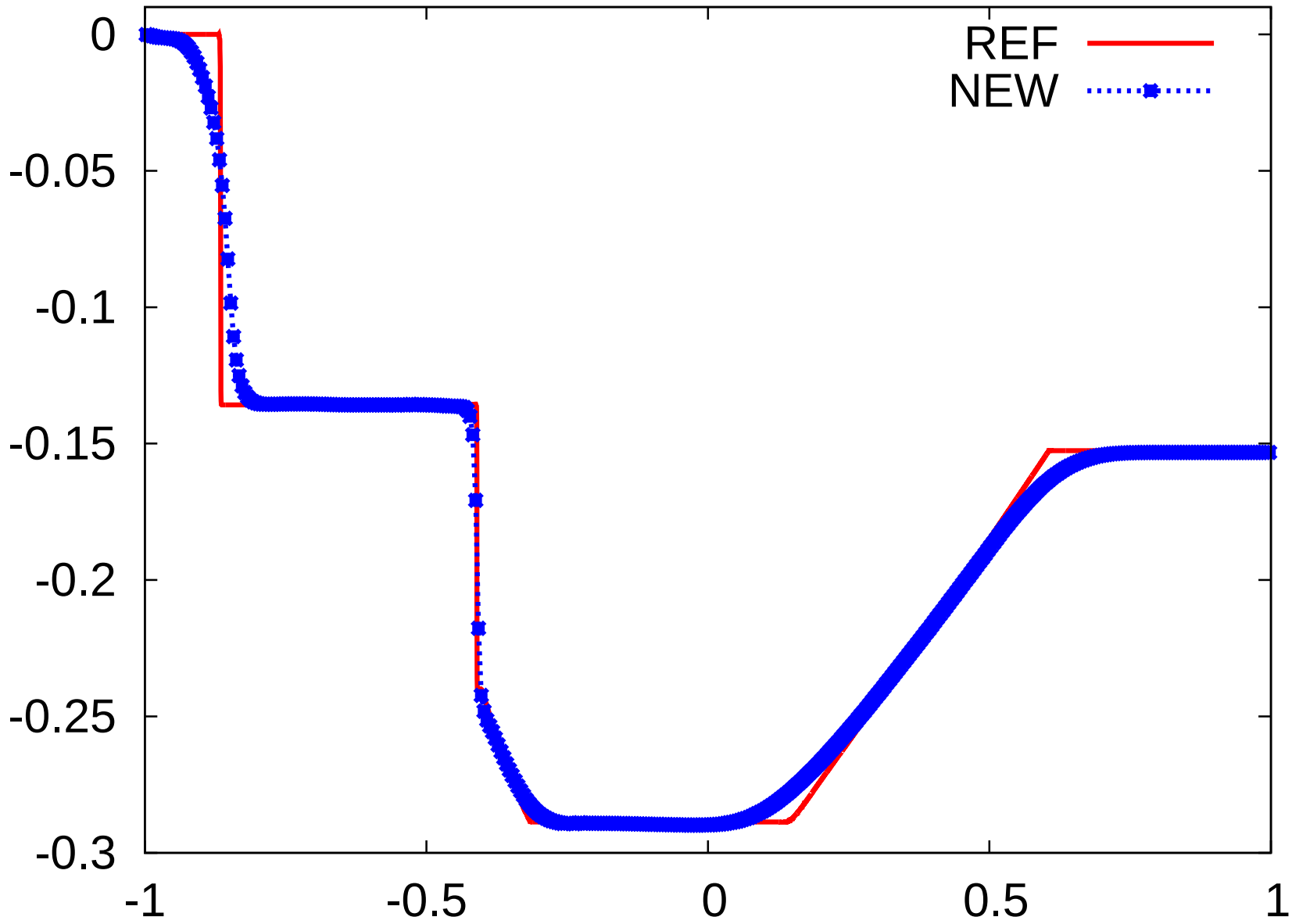

Pressure, $\Delta x = 1/200$